NAVAL POSTGRADUATE SCHOOL
Monterey, California

THESIS

ENVIRONMENTAL INFLUENCES ON THE PRODUCTION OF ARCTIC HALOCLINE AND DEEP WATER

by

James A. Hill

June 1988

Thesis Advisor Albert J. Semtner

Approved for public release; distribution is unlimited.

REPORT DOCUMENTATION PAGE

1a Report Security Classification: Unclassified		1b Restrictive Markings	
2a Security Classification Authority		3 Distribution Availability of Report: Approved for public release; distribution is unlimited.	
2b Declassification/Downgrading Schedule			
4 Performing Organization Report Number(s)		5 Monitoring Organization Report Number(s)	
6a Name of Performing Organization: Naval Postgraduate School	6b Office Symbol (*if applicable*): 35	7a Name of Monitoring Organization: Naval Postgraduate School	
6c Address (*city, state, and ZIP code*): Monterey, CA 93943-5000		7b Address (*city, state, and ZIP code*): Monterey, CA 93943-5000	
8a Name of Funding/Sponsoring Organization	8b Office Symbol (*if applicable*)	9 Procurement Instrument Identification Number	
8c Address (*city, state, and ZIP code*)		10 Source of Funding Numbers	
		Program Element No	Project No / Task No / Work Unit Accession No

11 Title (*include security classification*): ENVIRONMENTAL INFLUENCES ON THE PRODUCTION OF ARCTIC HALOCLINE AND DEEP WATER

12 Personal Author(s): James A. Hill

13a Type of Report	13b Time Covered	14 Date of Report (*year, month, day*)	15 Page Count
Master's Thesis	From To	June 1988	54

16 Supplementary Notation: The views expressed in this thesis are those of the author and do not reflect the official policy or position of the Department of Defense or the U.S. Government.

17 Cosati Codes			18 Subject Terms (*continue on reverse if necessary and identify by block number*)
Field	Group	Subgroup	Arctic, halocline, deep water, plume flow, polyna

19 Abstract (*continue on reverse if necessary and identify by block number*)

Pease (1987) related the effects of atmospheric forcing, mainly temperature and wind fields, to the size of coastal polynas. Using Pease's formulation and Killworth's (1977) plume model as applied by Melling and Lewis (1982), the effects of atmospheric forcing on brine injection into the Arctic pycnocline are investigated. This paper will discuss the likelihood of coastal polynas as a source for denser abyssal waters.

A standard case was developed for the model with initial conditions taken from Melling and Lewis (1982) and Pease (1987) for comparison with individual sensitivity experiments. Ten environmental parameters were individually examined for their influence on the plume depth after 90 days. The standard case resulted in a 90-day plume depth of 436 meters. A submarine canyon case was simulated, resulting in plume penetration to over 1300 meters in 90 days. Further experiments used actual T-S soundings from Aagaard et al. (1981) and Ostlund et al. (1987). Finally, a 20 kilometer wide plume is shown to penetrate to almost 600 meters in 90 days.

20 Distribution/Availability of Abstract: ☒ unclassified/unlimited ☐ same as report ☐ DTIC users	21 Abstract Security Classification: Unclassified	
22a Name of Responsible Individual: Albert J. Semtner	22b Telephone (*include Area code*): (408) 646-2768	22c Office Symbol: 54Ss

DD FORM 1473,84 MAR — 83 APR edition may be used until exhausted. All other editions are obsolete.

Approved for public release; distribution is unlimited.

Environmental Influences on the Production of Arctic Halocline and Deep Water

by

James A. Hill
Lieutenant, United States Navy
B.S., Sam Houston State University, 1979

Submitted in partial fulfillment of the
requirements for the degree of

MASTER OF SCIENCE IN METEOROLOGY AND OCEANOGRAPHY

from the

NAVAL POSTGRADUATE SCHOOL
June 1988

ABSTRACT

Pease (1987) related the effects of atmospheric forcing, mainly temperature and wind fields, to the size of coastal polynas. Using Pease's formulation and Killworth's (1977) plume model as applied by Melling and Lewis (1982), the effects of atmospheric forcing on brine injection into the Arctic pycnocline are investigated. This paper will discuss the likelihood of coastal polynas as a source for denser abyssal waters.

A standard case was developed for the model with initial conditions taken from Melling and Lewis (1982) and Pease (1987) for comparison with individual sensitivity experiments. Ten environmental parameters were individually examined for their influence on the plume depth after 90 days. The standard case resulted in a 90-day plume depth of 436 meters. A submarine canyon case was simulated, resulting in plume penetration to over 1300 meters in 90 days. Further experiments used actual T-S soundings from Aagaard et al. (1981) and Ostlund et al. (1987). Finally, a 20 kilometer wide plume is shown to penetrate to almost 600 meters in 90 days.

TABLE OF CONTENTS

LIST OF TABLES

LIST OF FIGURES

ACKNOWLEDGEMENTS

I would like to state my appreciation to Mr. Steve Ackley for his assistance and encouragement; Mr. Humphrey Melling, for his advice and for providing the numerical code of the streamtube model; the Oceanography research assistants (mainly Ms. Arlene Bird and Mr. Mike McCann) for their inexhautable resourcefulness thoughout my studies; and Professor Albert J. Semtner for his unflappable patience. Lastly, I would like to thank my family, Juanita, Patrick, and Corey for their support.

I. INTRODUCTION

The Arctic Ocean, a small and remotely located part of the world's ocean, has demanded the attention of those who wish to understand the Earth's climate. The renewed emphasis in recent years given to understanding the Earth's climate has underscored the role of the Arctic Ocean in the scheme of the global energy balance. The Arctic Ocean is also a key player in the world oceans' thermohaline circulation. Because of the importance of the Arctic Ocean in the global picture, understanding the nuances of the Arctic Ocean's physical oceanography and its sensitivities to environmental change is essential before climatologists, oceanographers, and meteorologists can develop a more realistic and longer range global climatological concept. Two puzzling aspects of the Arctic Ocean are its isothermal halocline and the more saline deep waters. How is the halocline maintained in a nearly horizontally independent state? What is the mechanism behind the formation of the Arctic Ocean's deep waters? These topics will be discussed in this thesis.

Throughout the Arctic Ocean, the characteristics of the upper layers are remarkably independent of the horizontal location of the sample. The water column consists of a mixed layer, halocline, thermocline, and deeper waters. The mixed layer is a relatively fresh water layer approximately 30 meters deep. River run-off and the summer cycle of melting ice are considered the main contributors to the fresh water layer. The halocline is the layer of water beneath the mixed layer. In this layer, salinities rise from 31 to as high as 34.6 ppt at the 200 meter depth level (Killworth and Smith, 1984). The halocline is, in essence, an isothermal layer with temperatures just above the freezing point. The thermocline is a layer below the halocline, in which temperatures rise to approximately 0° C at 250 meters (Melling and Lewis,1982) and continues to rise to 0.5° C at 400 meters due to the layer of warm Atlantic water. Below this depth, temperatures decrease with increasing depth. The deep waters of the Arctic Ocean are among the most dense waters found in the world's oceans and have been suggested as being an additional source for ventilating the world's oceans' deep thermohaline circulation (Aagaard,1981). Although the physical oceanography of the Arctic Ocean is well described in literature, the exact mechanism(s) for the maintenance of the halocline and deep water formation are not fully understood.

The halocline is generally isothermal except in the Canadian Basin, where warm Pacific waters entering via the Bering Strait causes a warm layer at about the 75-100 meter depths, and presents a paradox when examining its origin. Sandwiched between a cold, relatively fresh layer and a warm, saline layer, an obvious solution to the maintenance of the halocline might be simple vertical mixing between the two layers. However, vertical mixing of the cold, less saline surface water with the warmer, more saline Atlantic water is not considered to be a source since heat is not mixed along with salt. Aagaard et al. (1981) showed a discontinuity existed in the T-S correlation slope at about 150 meters. Either salinization of surface waters by freezing (i.e. brine rejection) or cooling of Atlantic water could be two possible mechanisms to produce halocline water. The authors (Aagaard, et al., 1981) demonstrate mixing between the two layers cannot be a source of halocline water by examining the required salinity of the surface water. Using a T-S diagram, and assuming linear mixing at a ratio of 3:2 (surface water to Atlantic water), the surface water would need to have a salinity of 34.7 ppt. Salinity this high has not been observed in the Arctic surface layer. Therefore, the maintenance of the Arctic halocline is generally thought to be attributable to lateral advection of cold, saline water from the continental shelves. The shelf waters are made more saline due to brine rejection associated with ice growth. Aagaard (1981) proposed that continental shelf areas where an annual growth of ice less than 2 meters is necessary to modify summertime salinity profiles to wintertime profiles may be the source areas of the halocline waters. Upwelling of Atlantic water onto the shelves and subsequent cooling has also been suggested as a possible source. Upwelling along submarine canyons has been reported as early as 1929 (Sverdrup,1929). As further evidence eluding to the halocline's possible shelfwater origin, water on the continental shelves has been shown to have temperature and salinity characteristics similar to the waters found offshore at a depth of 150 meters (Melling and Lewis, 1982).

In their paper, Melling and Lewis (1982) discuss the lateral advection of low temperature high salinity shelfwaters into the halocline, with particular attention paid to the effects of brine rejection due to the growth of ice. Aagaard (1981) used two methods of computing the necessary production rate of high salinity shelfwater to maintain the halocline. By considering the production rate required to renew the halocline in 10 years and necessary mixing ratios to achieve desired T-S characteristics, Aagaard suggests a $2.5x10^6$ to $4.0x10^6 m^3 - sec^{-1}$ for a production rate of cold saline shelfwater, assuming a halocline renewal period of 10 years. In order to increase the ambient shelfwater salinity

to values which would form sufficiently dense water to descend the slope into the halocline, Melling and Lewis (1982) emphasize the important role of ice dynamics, specifically the role of divergence. Areas of large wintertime ice cover divergence allow rapid ice growth hence increased salinization of the underlying water column. Leads and polynas are locations of rapid ice growth due to the divergence of the insulating ice cover.

Schumacher et al. (1983) examined the degree of salinization of the underlying water column beneath a polyna. In their study, measurements of salinity and water current velocity beneath a polyna located at St. Lawrence Island indicated polynas to be an area of high ice growth rates resulting in density driven currents due to increased salinization (Schumacher, et al., 1983). Coupling the salt source, i.e. polyna, with the interleaving plumes of dense shelfwater found by Melling and Lewis (1982) may provide a possible mechanism for the maintenance of the Arctic halocline. The polyna provides an atmospheric dependent source of salt into the water column possibly forming plumes which descend down into the halocline, as described by Melling and Lewis (1982). Along with the mechanism associated with the halocline's maintenance, the formation of the Canadian Basin's deep water has also been attributed to having a source of low temperature, high salinity shelfwater.

The dense waters which ventilate the world's oceans flow out of the Arctic Ocean over the Greenland-Scotland ridge system at a depth of about 2600 meters. A single source was advocated by Helland-Hansen and Nansen (1909) in which deep water is formed in the Greenland Sea. Nansen (1906) had written earlier of the possibility of the Greenland Sea Deep Water being modified by cooling in the Barents Sea. This theory omitted the possibility of deep water formation within the two basins of the Arctic Ocean, namely the Eurasian and Canadian Basins. In 1981, Aagaard postulated that deep water is also formed within the Arctic Ocean due to the salinity distribution. Greenland Sea Deep Water has a salinity of approximately 34.90 ppt, which is the least saline of Arctic deep waters. Therefore, at least two sources of deep water formation are thought to exist. One source is the traditional Greenland Sea formation area and the new source proposed by Aagaard, is within the Arctic Ocean's two basins.

The characteristics of water mass properties found in the Canadian and Eurasian Basins are similar until about the depth of the Lomonosov Ridge. At about 1500 meters depth, the Canadian Basin becomes more saline and is slightly warmer than the Eurasian Basin Deep Water (Aagaard, 1981). Under the traditional viewpoint of Greenland Sea

Deep Water filling the two basins through lateral advection, salinities should not exceed 34.9 ppt. However, during the LOREX (Lomonosov Ridge Experiment; Weber, 1979) salinities in the basins were determined to be greater than 34.9 ppt. This suggests an additional source of salt if not a completely new source of deep water. Current meters, placed over the Lomonosov Ridge, gave evidence to the existence of some tidal and other episodic surges carrying salinized Greenland Sea Deep Water over the ridge into the Canadian Basin. Even with the surges over the Lomonosov Ridge into the Canadian Basin, water from the Eurasian Basin must have an additional salt source to obtain the characteristics of water found in the Canadian Basin (Aagaard, 1981). Residence times can be calculated by comparing the mixing ratios of shelf water to Atlantic Intermediate water necessary to achieve the T-S characteristics found in the Canadian Basin Deep Water. Considering a small flux of shelfwater (.003 to .06 Sv) necessary to ventilate the Canadian Basin over several hundred years may also explain the warmer temperatures found in the Canadian Basin (Aagaard et al., 1985). By using tracers such as $\delta^{18}O$ and ^{14}C, Ostlund et al. (1987) agree with the magnitudes of the renewel time scales for both basins presented by Aagaard et al.(1985). Ostlund et al. (1987) and Aagaard et al. (1985) place the residence time of the Eurasian Basin in the order of decades vice several hundred years (700 years, Ostlund, et al., 1987) for the Canadian Basin. The requirement remains of an additional salt source at small fluxes to ventilate the Canadian Basin over several hundred years point to an episodic mechanism. Killworth and Smith (1984) write that shelfwater sinking at the basin edges may occur but a source of waters sufficiently dense to penetrate the Arctic Ocean's stable mid-layer remains a problem. Again, using a coastal polyna as a salt source, could shelfwater be modified under extreme conditions to produce such dense water which would then descend to the deeper depths via gravity flow plumes?

This thesis will combine Pease's numerical formulations relating atmospheric forcing, mainly wind and air temperature, to the opening and closing of coastal polynas, with a streamtube gravity flow model developed by Smith (1975). With simplified hydrography and suitable environmental conditions, this model can produce events of deep plume penetration along with a more consistent source of high salinity, low

temperature water for the maintenance of the Arctic Ocean's halocline. Chapter 2 will describe the numerical model used in this study along with an examination into drawbacks associated with Smith's streamtube model as described by other studies, i.e. Smith (1975), Killworth (1977), and Melling and Lewis (1982). Chapter 3 will describe results obtained by altering environmental inputs into the model and Chapter 4 will discuss the results and implications.

II. NUMERICAL METHODS AND PARAMETERS

A. THE NUMERICAL MODEL

With the increased desire to understand the nature of the Arctic halocline and its origin, there existed sufficient pieces of the puzzle to develop a coupled model. The 3-D turbulent entraining plume model developed by Smith (1975) has been used by several studies (Killworth (1977), Killworth and Carmack (1978), and Melling and Lewis (1982)) to gain insight into gravity flow currents arising from brine rejection into the water column due to ice growth. Melling and Lewis (1982), compute the initial density of the plume by estimating the average ice grown annually in a shallow shelf and and the resultant salinity contribution. In this study, Pease's (1987) formulation relating a polyna's size to offshore wind speed and air temperature, provides a specific source of brine which is then coupled with Smith's plume model, as used by Melling and Lewis (1982), in order to study the possible contribution of the polyna produced denser waters to the Arctic halocline and possible formation of Canadian Basin Deep Water.

1. The coastal polyna

Pease (1987) describes the polyna's maximum width as an equilibrium between frazil ice production and its advection rate. The frazil ice production rate is a function of the heat exchange at the air-sea interface. Therefore, with wind speed and air temperature as independent variables, one can compute the size of the polyna and its frazil ice production rate.

The polyna size can be found by solving:

$$\frac{dX}{dt} = V_i - \frac{X_p F_i}{H_i} \tag{1}$$

where $\frac{dX}{dt}$ is the change in polyna width with time, V_i is the advection rate of frazil ice, X_p is the polyna width, F_i is the frazil ice production rate, and H_i is the collection depth of grease ice or nilas. The solution of equation (1) assumes the meteorological conditions are steady throughout the polyna's opening time, thus allowing treatment as a linear differential equation. Furthermore, if the meteorological event is assumed to be

of sufficient duration so that the polyna reaches maximum width, equation (1) can be written as:

$$X_p(maximum) = \frac{V_i H_i}{F_i}. \tag{2}$$

This allows solving equation (2) for the maximum width after computing the frazil ice production rate, F_i. In this study, meteorological events of interest are 4-10 days duration, therefore this assumption allowing equation (2) is valid. Ou (1988) describes a more detailed coastal polyna model and concludes the ice edge is less affected by higher frequency atmospheric disturbances than longer period, synoptic type variations. Although Ou (1988) includes additional physics to model the temporal changes of the polyna's ice edge, the steady state solution is still that as given by Pease (1987) and shown above in equation (2).

The frazil ice production rate is given by Pease (1987) as:

$$F_i = -\frac{[\sigma e_a T_a^4 - Q_{lu} + \rho_a C_h C_p V_a (T_a - T_w)]}{\rho_i L} \tag{3}$$

where the evaporative heat flux has been neglected due to its small contribution relative to the uncertainty of the sensible heat flux. Q_{lu} is the upward longwave radiation, $\sigma e_a T_a^4$ is the downward longwave radiation, L is the latent heat of freezing for salt water, ρ_i is the density of young sea ice, and $\rho_a C_h C_p V_a (T_a - T_w)$ is the sensible heat flux.

2. Salinity distribution within the water column

The salinity contribution to the water column from frazil ice growth is assumed to be uniform with depth and is computed using:

$$S_{new} = \overline{S} + \frac{(\overline{S} - S_i) F_i A_s}{\{\int q dz\}} \tag{4}$$

from Killworth and Smith (1984). S_{new} is the new salinity value of the water column after brine rejection. $\overline{S}$ is the average salinity of the shelfwater, S_i is the salinity of the ice, A_e is the effective area of salinization, and $\int q dz$ is the areal flux of the underlying water. Using F_i from the polyna model, one can compute the salinity of shelfwater exiting a polyna.

3. Equation of state

The density of the current is computed using the International one atmosphere equation of state developed by Millero and Poisson (1981). The equation is given below.

$$\rho = \rho_o + AS + BS + CS \tag{5}$$

where,

$$A = 8.24493 \times 10^{-1} - 4.0899 \times 10^{-3} t + 7.6438 \times 10^{-5} t^2 - 8.2467 \times 10^{-7} t^3 + 5.3875 \times 10^{-9} t^4$$

$$B = -5.72466 \times 10^{-3} + 1.0227 \times 10^{-4} t - 1.6546 \times 10 - 6 t^2$$

$$C = 4.8314 \times 10^{-4}$$

and ρ_o is the standard density of seawater. This allows the calculation of the current's relative buoyancy using:

$$\Delta_o = -\hat{g}\left(\frac{\rho_1 - \rho_2}{\rho_o}\right). \tag{9}$$

In this fashion, the results from the polyna model can be used as inputs to the streamtube model.

4. **The streamtube model**

Smith's (1975) model of boundary currents includes the effects of friction, entrainment, and Coriolis forces. The 3-D plume was modified by Killworth (1977) by altering the entrainment rate. Killworth (1977) related the entrainment rate to the product of the plume's area and velocity vice only the velocity (Smith, 1975). Melling and Lewis (1982) used Killworth's version of the plume model with an entrainment coefficient dependent on the Richardson number. The model used in this paper is the

Melling and Lewis (1982) adaptation with the inclusion of several stratified layers to allow a single model initialization.

Smith's plume model uses two coordinate systems. The Cartesian system is aligned with the bottom so the X-axis lies along the shore and the Y-axis lies along the slope. The second coordinate system is the curvilinear system with ξ and η axes. The position of the plume axis can be defined by the value of ξ . The angle which the plume crosses the isobaths is given by the angle β . The coordinate system is illustrated in Figure 1 on page 10 and includes gravitational, $\hat{g}$, and rotational, Ω, vectors.

The equations for the path flow are:

$$\frac{dX}{d\xi} = \cos\beta \tag{10}$$

and

$$\frac{dY}{d\xi} = \sin\beta. \tag{11}$$

The plume is considered to be a well-mixed, broad, thin layer of high density fluid adjacent to the bottom. Pressure gradient forces pull the plume down the slope while Coriolis forces bend the flow to the right. If frictional forces were not considered, the flow would move horizontally along the isobaths (Killworth, 1977) in geostrophic balance. Friction is included, using quadratic drag laws to relate frictional resistance to the square of the mean velocity (Smith, 1975). The plume is thus allowed to flow down the slope, constantly entraining ambient fluid and losing its negative buoyancy. Once the plume reaches neutral buoyancy, the plume interleaves with the ambient waters. The equations of the plume's flow from Killworth (1977), are:

$$\frac{d}{d\xi}(AV) = E_1 A^{\frac{1}{2}} V, \tag{12}$$

$$\frac{d}{d\xi}(AV^2) = A\Delta \sin\theta \sin\beta - K_1 A^{\frac{1}{2}} V^2, \tag{13}$$

$$\frac{d}{d\xi}(AV\Delta) = -AVN^2 \sin\theta \sin\beta, \tag{14}$$

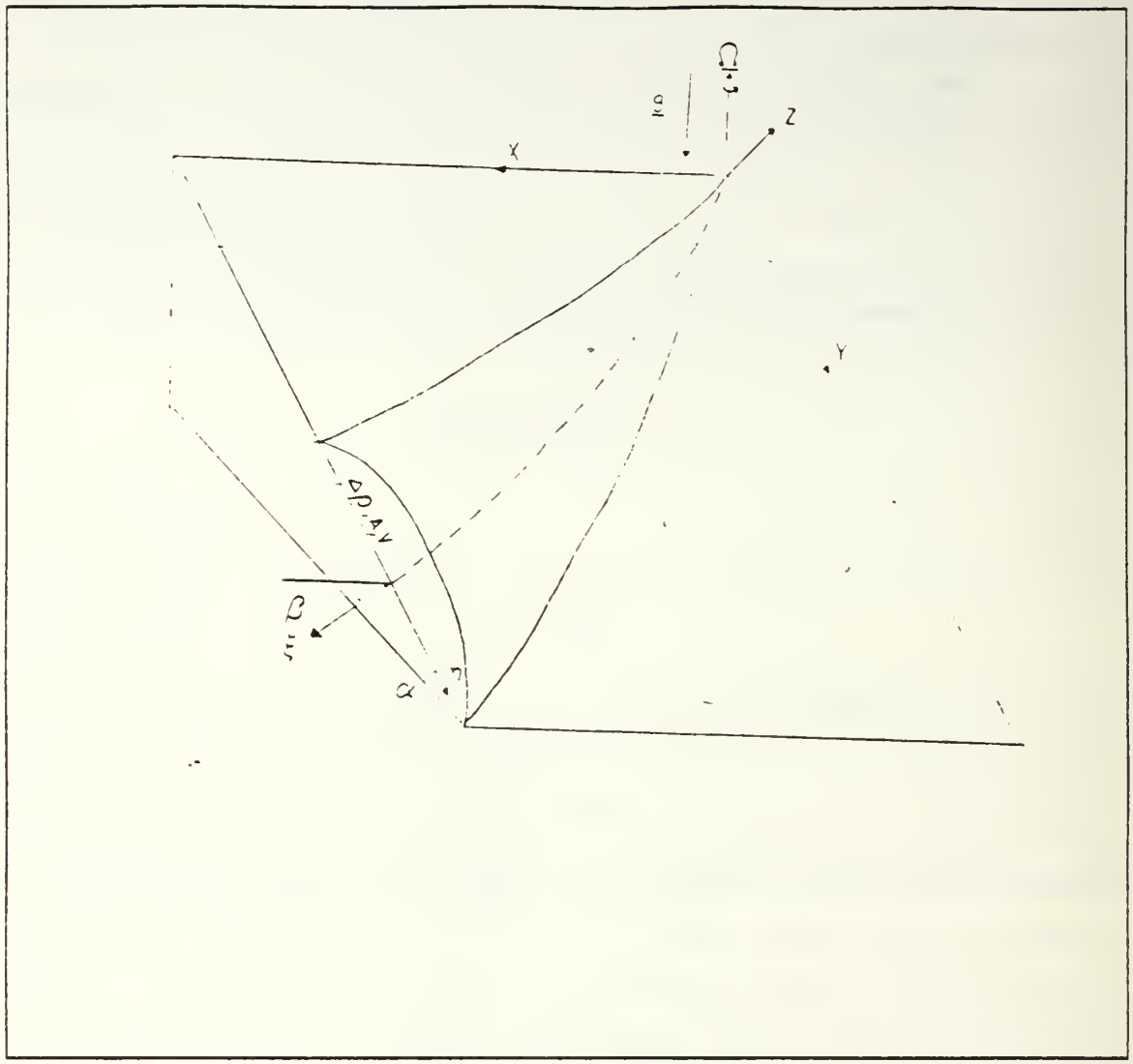

Figure 1. The streamtube coordinate system as given by Smith (1975).

$$V^2 \frac{d\beta}{d\xi} = \Delta \sin\theta \cos\beta - fV. \tag{15}$$

These equations are, the along-stream derivatives of the mass flux (12), the momentum flux (13), the buoyancy flux (14) and the cross stream momentum balance (15). In the above equations, A is the cross-sectional area of the plume, V is the plume's velocity, Δ is the plume's buoyancy, θ is the slope angle, β is the angle at which the plume crosses

the isobath, N is the Brünt-Väisälä frequency, K_1 is the drag coefficient, f is the Coriolis parameter, and E_1 is the entrainment coefficient.

The equations were integrated using a modified Adams method.

Predictor:

$$y_{i+1} = y_i + \frac{h}{24}(55f_i - 59f_{i-1} + 37f_{i-2} - 9f_{i-3}) \tag{16}$$

Corrector:

$$y_{i+1} = y_i + \frac{h}{24}(9f_{i+1} + 19f_i - 5f_{i-1} + f_{i-2}), \tag{16a}$$

with the initial steps provided with the Runge-Kutta method,

$$\begin{aligned} y_{i+1} &= y_1 + \frac{h}{6}(k_1 + 4k_2 + k_3) \\ k_1 &= f(x_i, y_i) \\ k_2 &= f(x_i + \frac{h}{2}, y_i + \frac{h}{2}k_1) \\ k_3 &= f(x_i + h, y_i - hk_i) \end{aligned} \tag{18}$$

This model uses Killworth's (1977) entrainment and frictional parameterizations, which has the entrainment rate and frictional force porportional to the product of the area and velocity (velocity squared for friction). Thus, $\frac{E}{E_1} = \frac{K}{K_1} = (\frac{w}{b})^{\frac{1}{2}}$, where w is the width of the plume and b is the depth of the plume. Also used in this model is Bo Pedersen's (1980) entrainment parameterization for small slopes. Melling and Lewis (1982) included this in their version of Smith's model. The entrainment coefficient is given as $E = 0.072 \sin\theta \sin\beta = 0.072(\frac{K}{Ri})$ where $Ri = b\Delta \cos\theta / V^2$ is the bulk Richardson number of the flow.

5. The coupled model

The model takes the form illustrated in Figure 2 on page 13. Underneath the polyna, a plume with a depth, b, and a width, w, is salinized due to brine rejection. The plume has an initial velocity, V_o. The effects of varying the initial velocity will be examined in Section 3, however, the standard case value of $V_o = .04 m/s$ is used. This value

is close to the values used by Melling and Lewis (1982) and observed values of currents adjacent to polynas reported by Schumacher et al. (1983). The value of V_o determines the areal flux used in calculating the salinity increase in the water column. The initial velocity is increased after the non-entraining, non-rotating rudiment plume travels 10 km straight downslope. Effects of rotation are neglected at this early stage of the plume to minimize the exposure to brine rejection under the polyna. Increasing the velocity after 10 km ensures more realistic salinity values of the plume, and would, in any case, occur in the first steps of the streamtube model. The non-entraining, non-rotating rudiment plume continues straight downslope until a depth of 45 meters is reached. This depth was chosen due to its use by Melling and Lewis (1982) as the initial depth of the streamtube model.

At 45 meters, the plume descends the slope according to the dynamics set forth and established by Smith (1975), Killworth (1977), and Melling and Lewis (1982). Three stratified layers are defined in this coupled model. Layer 1 lies between 45 and 55 meters depth, Layer 2 lies between 55 and 300 meters, and Layer 3 lies below 300 meters. The plume is assumed to interleave with ambient waters when the velocity is less than .01 m/s; however, all sensitivity studies will be carried out using 90 days as the maximum number of days the plume can descend while retaining its integrity.

B. MODEL PARAMETERS

1. Environmental variables

In order to examine the environment's influence upon possible polyna- related production of halocline and deep waters, certain environmental variables were individually varied during model simulations. The sensitivity of the model to a variable's alteration is defined by the dependence of the plume's depth after 90 days upon the particular variable, relative to a standard case. The relationship between the depth of the plume and a single environmental variable will be reported in Chapter 3. The variables to be investigated are listed in Table 1 on page 14.

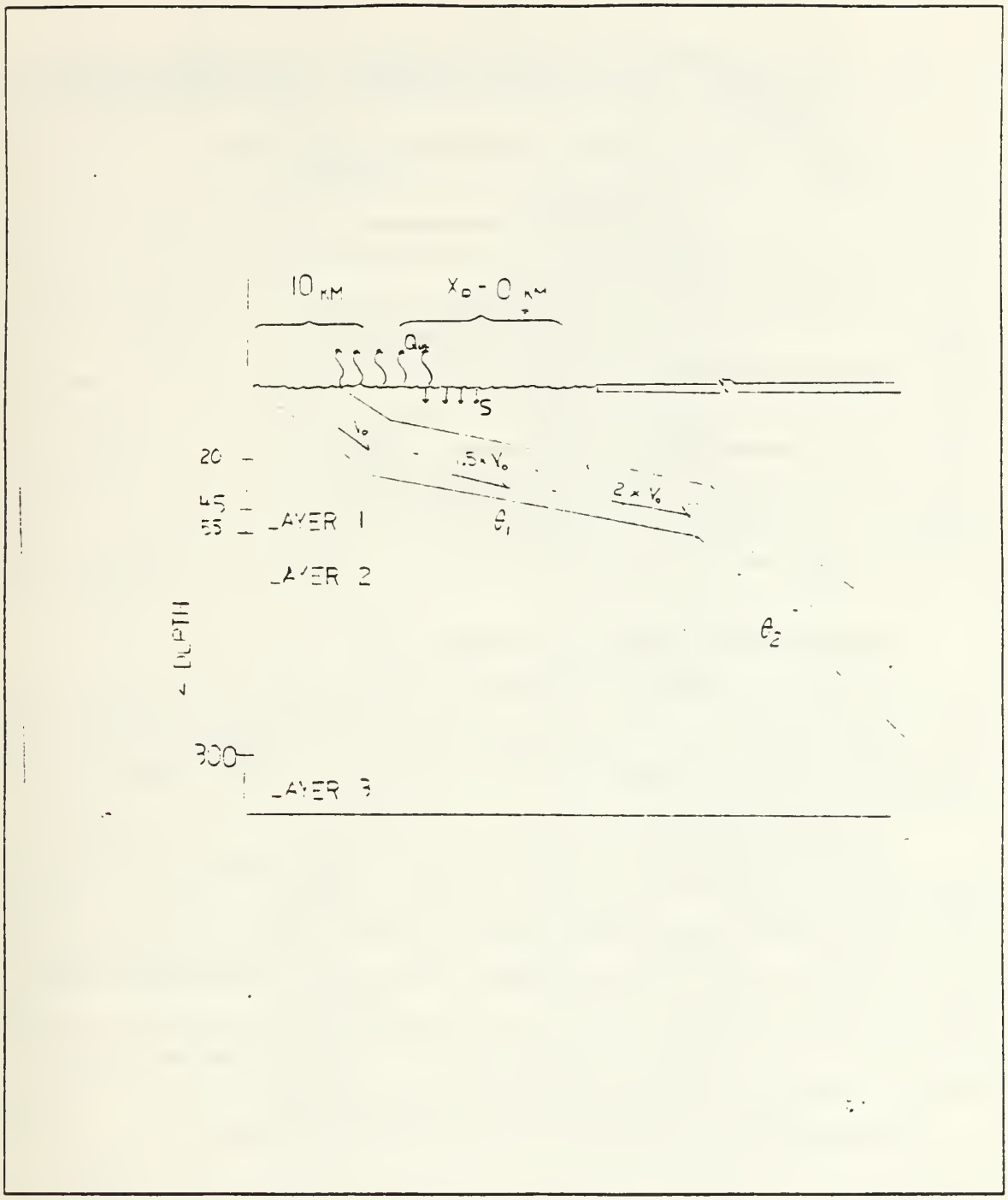

Figure 2. Schematic representation of the coupled model. As the shelfwater is exposed to the polyna, a high density plume is formed, resulting in the plume's descent down the slope until it is neutrally buoyant.

Table 1. **LIST OF ENVIRONMENTAL INPUTS:** The dependency of the plume depth after 90 days on each of the variables below will be examined in Section 3.

Variable	Definition.
T_{air}	air temperature
V_a	wind velocity
$\overline{S}$	shelfwater salinity
V_o	initial shelfwater velocity
Sw	shelf width, from the 45 m isobath
θ_1	initial shelf slope
θ_2	secondary slope
N_1	Brünt-Väisälä frequency, layer 1
N_2	Brünt-Väisälä frequency, layer 2
ΔZ_2	thickness of layer 2

2. Environmental conditions for the standard case

To achieve consistency with pre-existing works, many of the environmetal conditions for the standard case were borrowed from Melling and Lewis (1982), Killworth and Smith (1984), and Pease (1987). The standard case initial values are listed in Table 2 on page 15.

The most significant departure from an initial value given by previous work, is the H_i value. In this paper, the frazil ice collection thickness is taken to be .2 meters. Pease (1987) shows a higher collection thickness results in longer polyna opening time and larger polyna width for the same wind speed and air temperature. Weeks and Ackley (CRREL Monograph 82-1, 1982) give higher values for frazil ice collection thicknesses in a wind driven scenario vice .01 to .1 meters in quiescent conditions. In addition to the frazil ice collection thickness, the salinity of the ice is set to 7 ppt (Cox and Weeks, 1974) instead of 5 ppt used in Killworth and Smith (1984).

Table 2. INITIAL VALUES USED FOR THE STANDARD CASE.

Variable	Value	Definition
T_{air}, °C	-15.	air temperature
T_w, °C	-1.8	water temperature
V_{air}, $m\ sec^{-1}$	15.	wind velocity
V_i, $m\ sec^{-1}$	3 % V_{air}	ice floe velocity
H_f, m	.2	frazil collection thickness
σ, $Wm^{-2}deg^{-4}$	$5.67x10^{-8}$	Stephan-Boltzmann constant
e_a	0.95	emissivity of the air
ρ_a, kgm^{-2}	1.30	air density
ρ_w, kgm^{-3}	$1.026x10^{3}$	seawater density
ρ_i, kgm^{-3}	$0.95x10^{3}$	ice density
C_h	$2.0x10^{-3}$	sensible heat coefficient
C_p, $Jdeg^{-1}kg^{-1}$	1004	specific heat of air
Q_{lu}, Wm^{-2}	301	longwave radiation upward
L, Jkg^{-1}	$3.34x10^{5}$	latent heat of fusion
b_0, m	10.	flow thickness
w_0, m	1000.	flow width
V_0, $m\ sec^{-1}$	.04	flow speed
β, degrees	29	flow direction
f, sec^{-1}	$1.38x10^{-4}$	Coriolis parameter
N, sec^{-1}	0.0316	Brünt-Väisälä frequency, layer 1
N	0.0077	Brünt-Väisälä frequency, layer 2
N	0.001	Brünt-Väisälä frequency, layer 3
ΔZ_2, meters	195	Layer 2 thickness
θ_1	$0.5x10^{-3}$	initial bottom slope
θ_2	$5x10^{-3}$	secondary bottom slope
K	0.01	drag coefficient
E	$0.072 \sin\theta \sin\beta$	entrainment coefficient
$\bar{S}$, ppt	32.5	initial shelfwater salinity
S_i, ppt	7.0	Salinity of frazil ice

III. RESULTS

A. STANDARD CASE

In order to examine the environmental influence on the possible polyna production of halocline and deep waters, a standard case was defined with values which are typical of Arctic Ocean observations. The offshore wind velocity requires a considerable meteorological event providing winds higher than the monthly mean winds. However, the value of 15 m/s for offshore wind velocity is within observed wind speeds for Arctic storms reported in previous papers (Schumacher, et al. (1983) and Aagaard, et al. (1985)). The standard case plume obtains a salinity of 34.98 ppt after transversing the polyna, which corresponds to a density of 1032.93 gm/m^3 and a negative buoyancy of .0643 m/s^2 . It is therefore not suprising when the plume penetrates the same Arctic pycnocline used in Melling and Lewis (1982) to a depth of 436 meters. Figure 3 on page 17 shows the velocity of the plume as it descends the slope. Due to the plume's high negative buoyancy, the plume accelerates slightly on the initial slope then rapidly increases in speed after the shelf break at 55 meters. The maximum velocity is 0.30 m/s reached at a depth of 60 meters. The mass flux, AV, increased by over 1600% emphasizing the dependence of the entrainment rate on the velocity of the plume. At the end of 90 days, the standard case plume has a velocity of 0.017 m/s and a negative buoyancy of 0.000482 $m/$ sec^2. The plume has travelled 253 kilometers along the shoreline and 96 kilometers down slope. The flow path of the plume can be seen in Figure 4 on page 18. Overall, the plume in the standard case behaves similarly, although with different magnitudes, as the plumes in Melling and Lewis (1982). With this in mind, sensitivity studies of the impact of individual environmental parameters on the 90-day plume depth can be examined. Sensitivity experimental results typically include 10-20 data points with increased resolution in areas of abrubt change.

B. SENSITIVITY EXPERIMENTS

The polyna's maximum width is dependent on the growth rate of ice, the advection rate of ice, and the collection thickness of ice. Air temperature and the wind speed affects the growth rate of ice, while the advection rate is proportional to the wind speed. Lowering the air temperature results in a monotonic increase in the plume's depth at 90 days as shown in Figure 5 on page 20. This is expected due to the increased production of frazil ice resulting in higher salinization of the water column. Although Pease (1987)

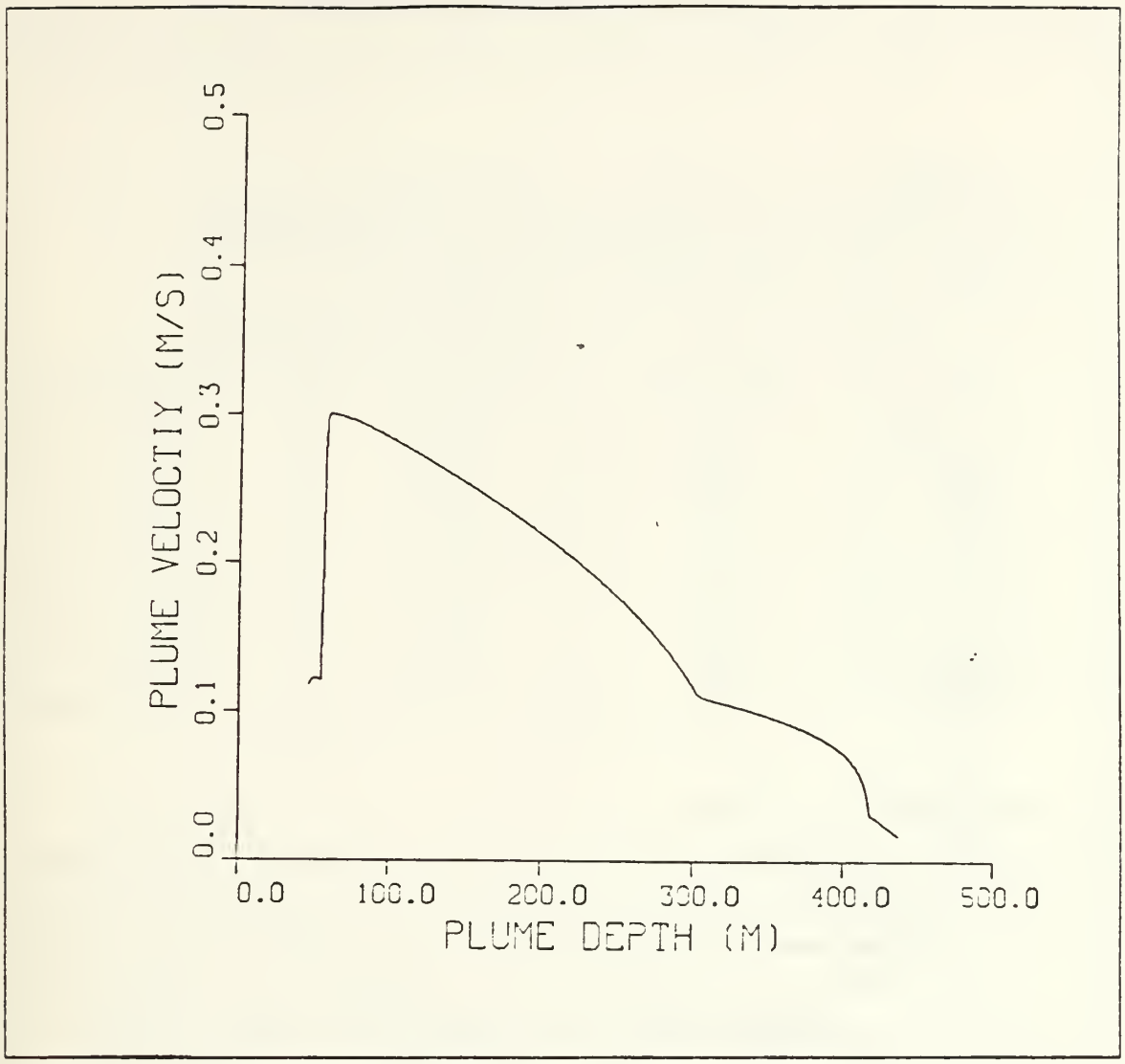

Figure 3. The standard case plume's velocity is shown with depth: Note the rapid increase in velocity as the plume crosses the shelfbreak at the 55 meter isobath to a steeper slope.

has shown the polyna size decreases with lowering air temperature at a given wind speed, the plume's salinity (hence, density) increases most rapidly in the first 10 kilometers of downslope travel. Here the plume will be subjected to significantly higher salinization due to higher ice growth rate and lower areal flux rate. Although the polyna size is smaller with lowering air temperatures, the majority of the salinization has already occurred in the first 10 kilometers. Indeed, the polyna shows a decreasing salt contribution

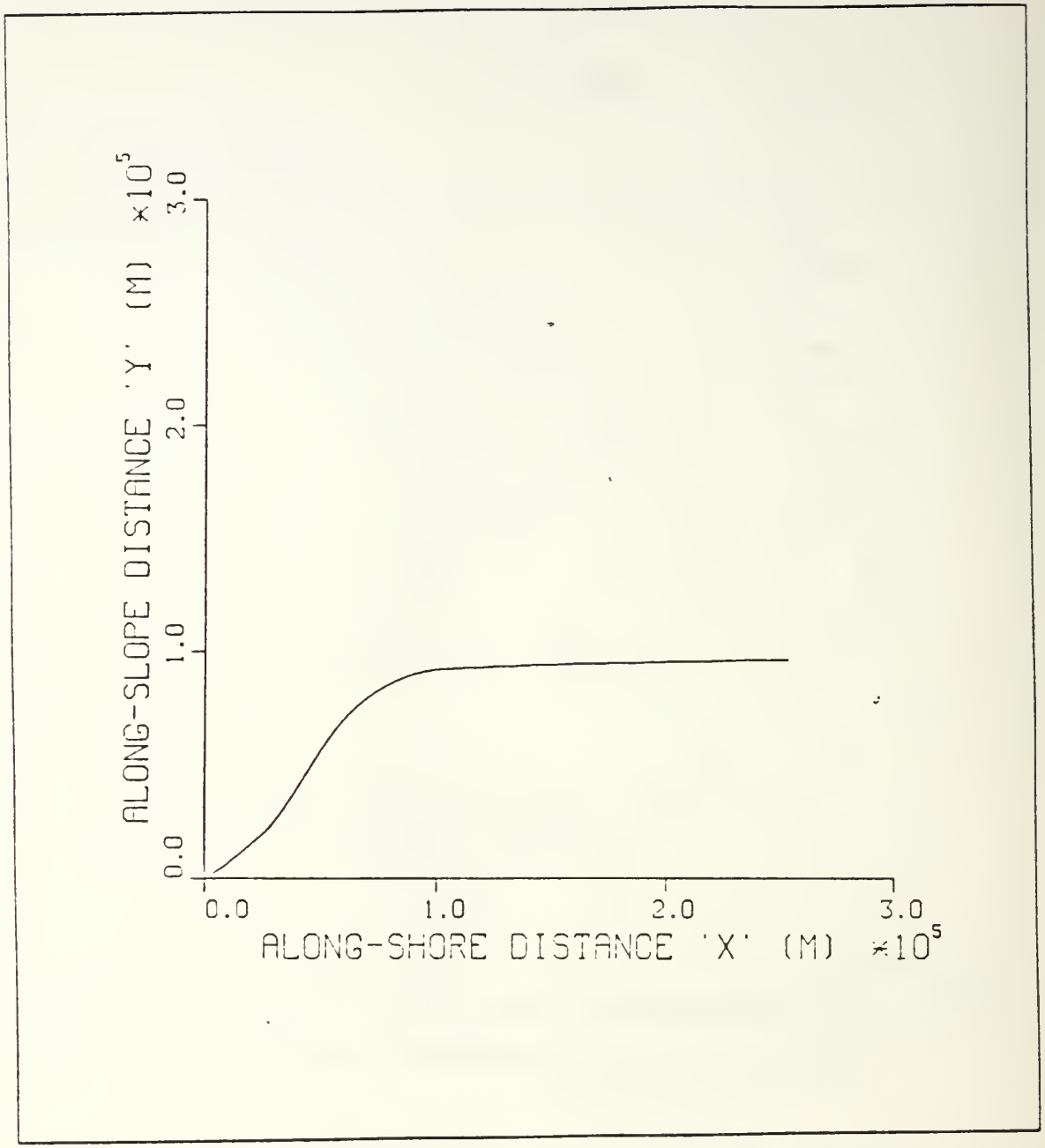

Figure 4. The standard case plume flow path in the *x*-*y* coordinates: The effects of Coriolis can be seen as the plume's angle β decreases during the plume's descent.

after the first 10 kilometers with decreasing air temperature. This can be seen in Table 3 on page 19. This decreasing salt contribution to the water column is due to the polyna's smaller width.

Table 3. **SALINITY CONTRIBUTION OF POLYNA WITH DECREASING AIR TEMPERATURE:** The table shows the initial salinity of the plume, S_{init}, after the first 10 kilometers of downslope travel, the final salinity of the plume, S_f, after travelling the entire width of the plume, X_p, and the decreasing salt contribution of the polyna during the distance $X_p - 10km$ with decreasing air temperature, T_{air}.

S_{init} , ppt	S_f , ppt	ΔS , ppt	T_{air}, ° C
33.36	34.36	1.0	-5.0
33.75	34.67	0.92	-10.
34.14	34.98	0.84	-15.
34.54	35.30	0.76	-20
34.93	35.61	0.68	-25
35.32	35.92	0.60	-30
35.72	36.23	0.51	-35

On the other hand, if air temperature is held constant, and offshore wind speed is increased, the polyna grows in size due to increased ice advection rate. The initial contribution of salt during the first 10 kilometers of the polyna does not vary however, the increased polyna size exposes the water column to further salinization. This results in a denser, deeper penetrating plume with increasing wind speed. (See Figure 6 on page 21). The dependence of plume depth upon the wind velocity and air temperature illustrate the possible atmospheric influences upon the Arctic Ocean's salinity characteristics. The frequency and severity of Arctic storms which would be conducive to high density plume formation is a consideration in the calculation of production rates, but cannot be discussed quatitatively using this simplified model.

The effect of varying the initial salinity of the shelfwater on plume depth is shown in Figure 7 on page 22. The results of this experiment show deeper penetration with higher initial salinity. This is not suprising due to the significant role of salinity upon water density near the freezing point. The plume depth after 90 days is greater than the depths reported by Melling and Lewis (1982), even with relatively low salinity values.

Initial shelfwater velocity defines two parameters within the model, the areal flux used in computing the new salinity of the water column and the initial velocity of the

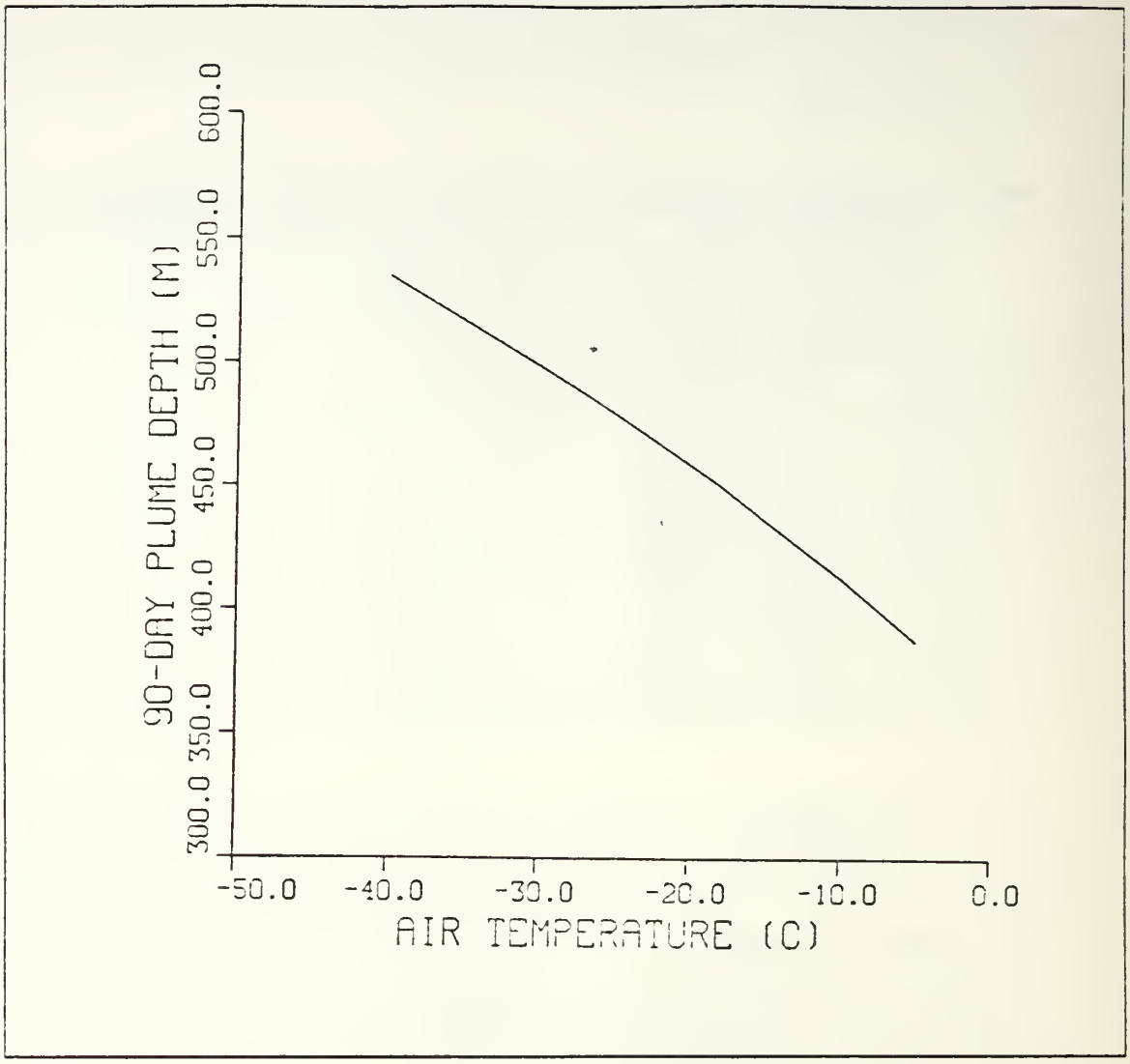

Figure 5. Effect of decreasing air temperature on the plume's 90-day depth: With decreasing air temperature, the increased ice growth rate results in higher initial salinization of the water column.

plume. The higher the initial velocity, the less saline the plume. However, when using the plume depth at 90 days as a standard criteria to examine the results, the higher velocity plumes reach deeper depths at 90 days than the denser, but lower velocity plumes. If a speed criteria were used, then there would be a negative correlation between the plume depth and initial shelfwater velocity. Instead, Figure 8 on page 23 shows a positive correlation between plume depth and initial shelfwater velocity.

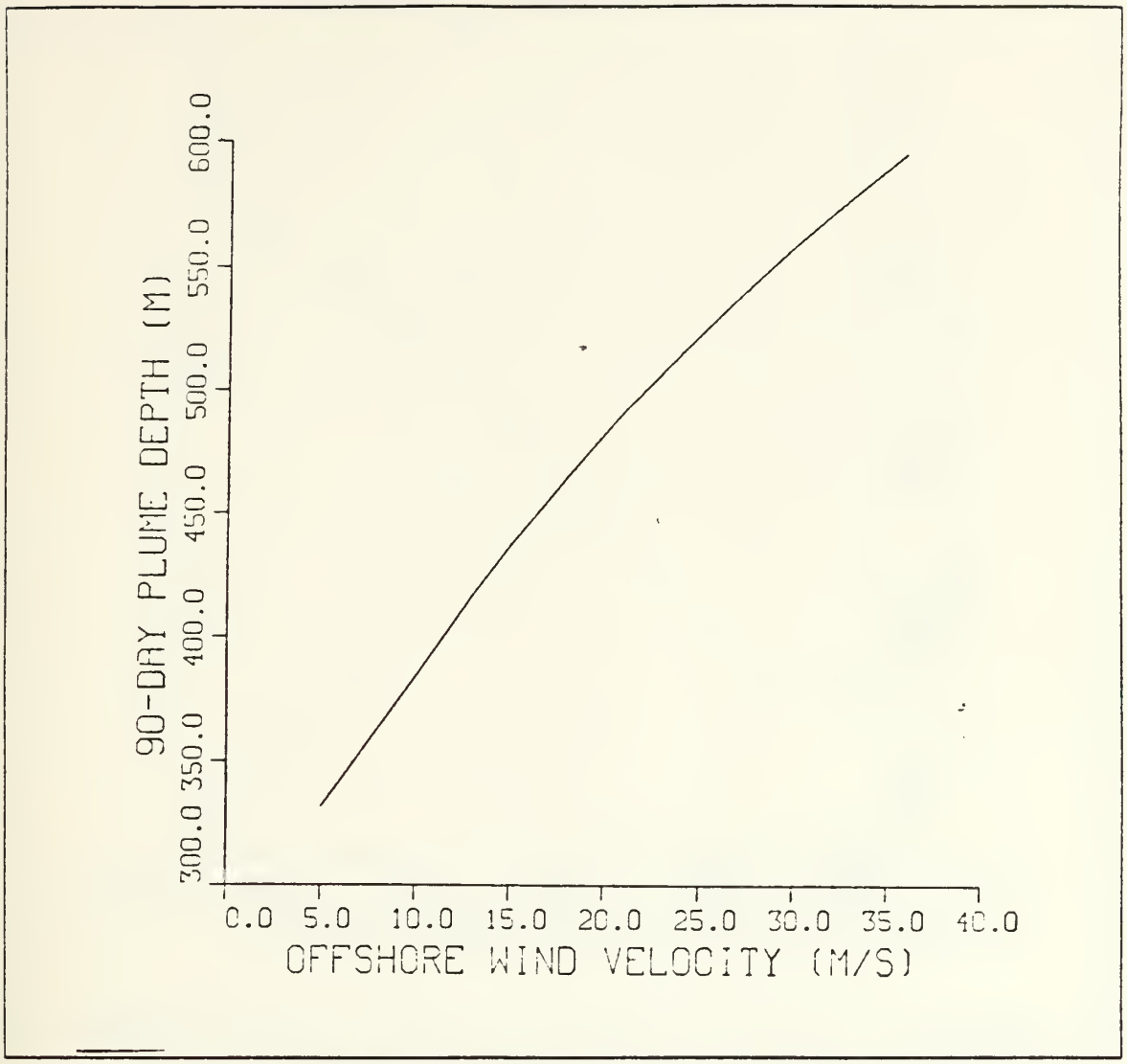

Figure 6. Effect of varying offshore wind speed on the 90-day plume depth: The polyna's increased width with increasing wind speed results in a higher density plume due to longer exposure of the water column to the polyna's brine rejection. This results in a deeper penetrating plume.

Similarly, the parameters of shelf slope and secondary slope appear to have contradictory results. Figure 9 on page 24 shows as the initial shelf slope is lessened, the plume penetrates to deeper depths after 90 days of travel. In this experiment, the shelf width was fixed at 20 kilometers after the 45 meter isobath. This deeper penetration appears to be due to a lower entrainment parameter, which is a function of the shelf

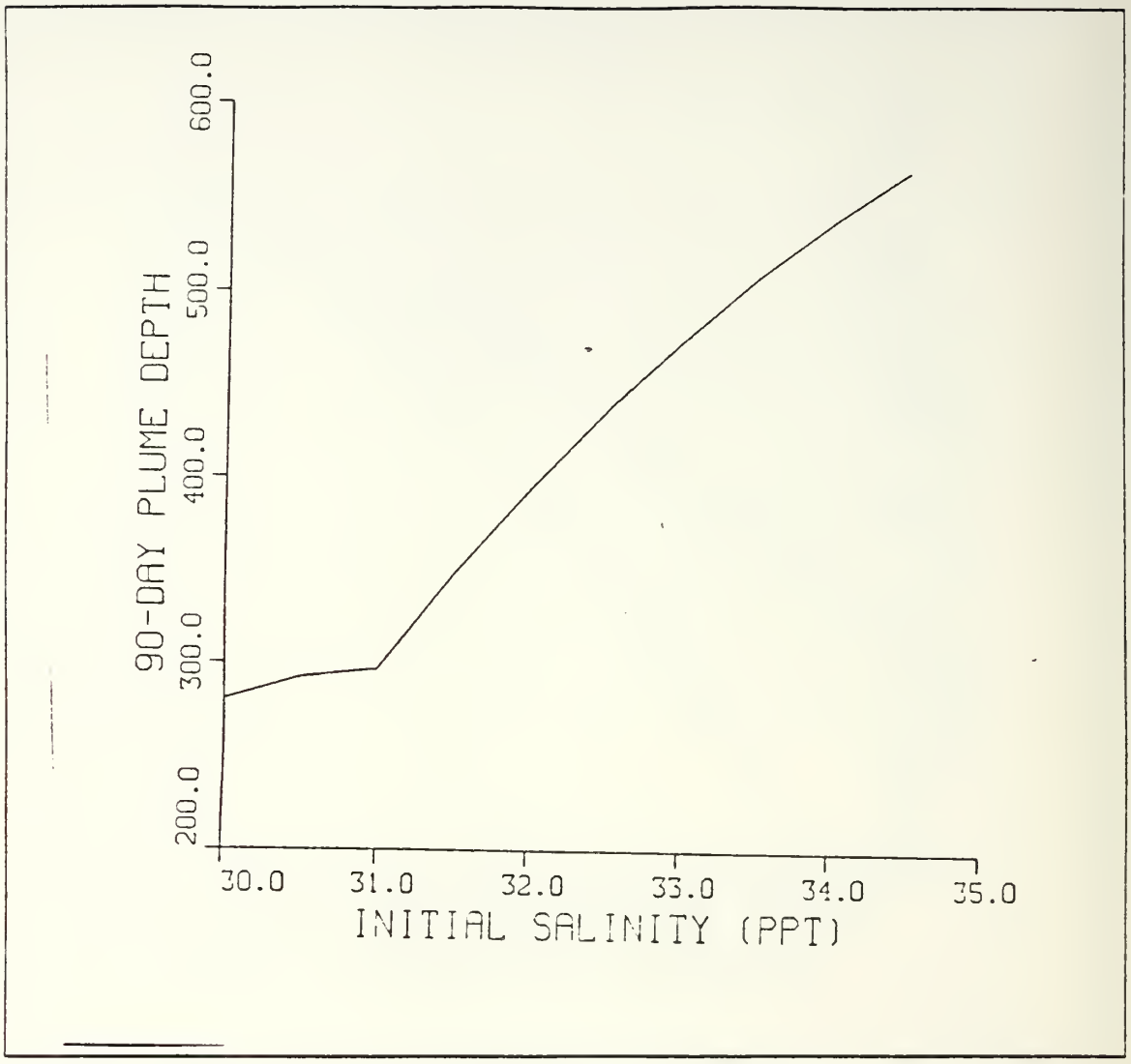

Figure 7. The effect of initial shelfwater salinity on the 90-day plume depth: With increasing shelfwater salinity the plume attains a higher density due to increased salt rejected by ice growth added to the shelfwater.

slope. In contrast, Figure 10 on page 25 shows deeper penetration with an increased secondary slope. Although the entrainment parameter still increases with slope, the 90-day plume depth is limited by the slope itself. Since 90 days was considered a reasonable time scale for the plume to maintain its integrity, deeper plume penetrations would most likely occur with steeper slopes after the shelf break, i.e. in submarine

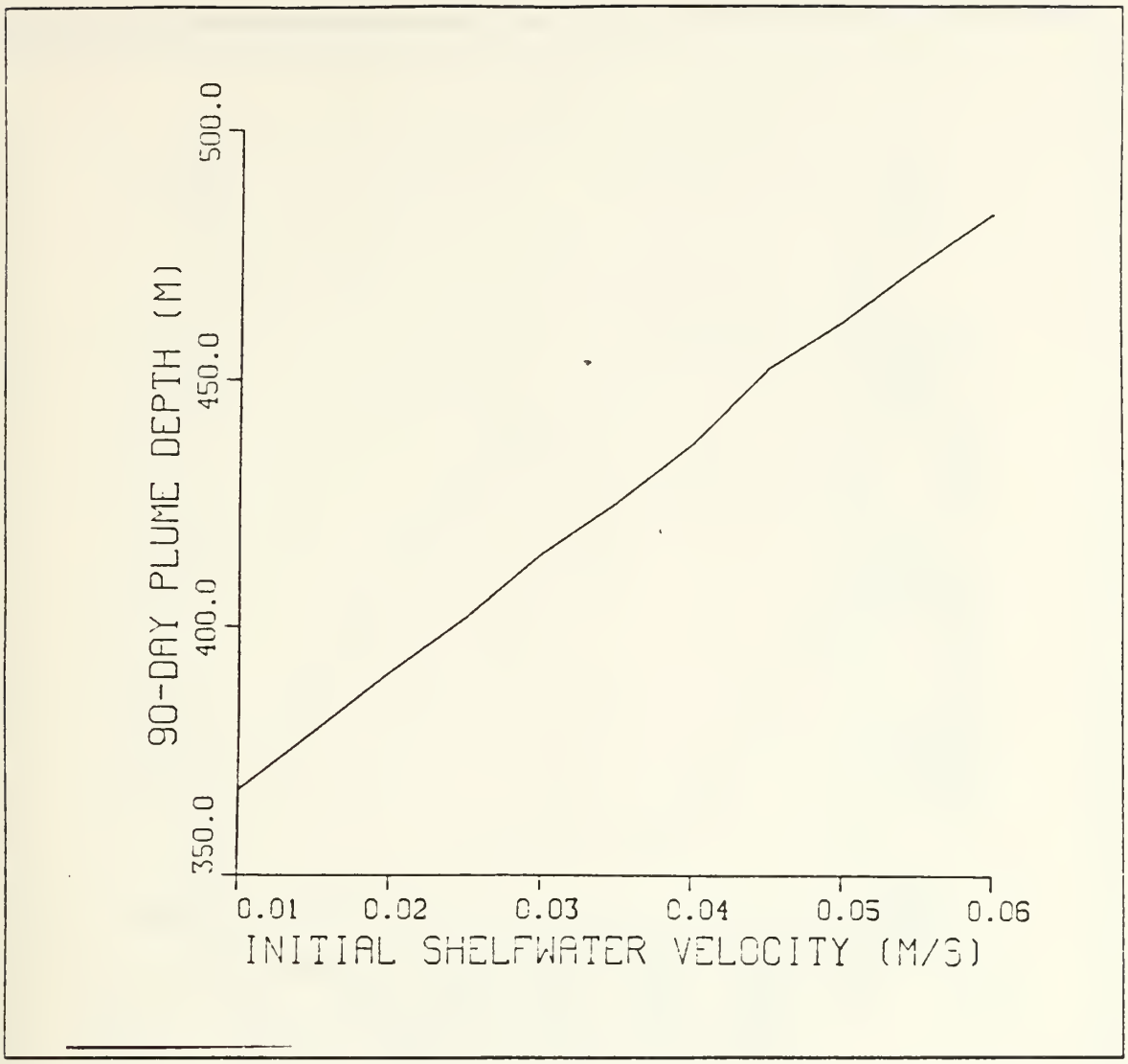

Figure 8. Effect of varying initial shelfwater velocity on 90-day plume depth: An increased initial velocity results in a deeper penetrating plume at 90 days.

canyons. Varying the shelf width after the 45 meter isobath has little effect on the 90-day plume depth. This is shown in Figure 11 on page 26.

Examining the stratification of the Arctic Ocean is accomplished by varying the Brünt-Väisälä frequency of Layers 1 and 2. The deep Layer 3 remains constant at a value used in Killworth (1977) for deep waters. Layer 1 is the initial pycnocline and represents the transition from the fresh surface layer to the saltier halocline. Figure 12 on page 27 shows the 90 day plume depth is little changed even with a substantially

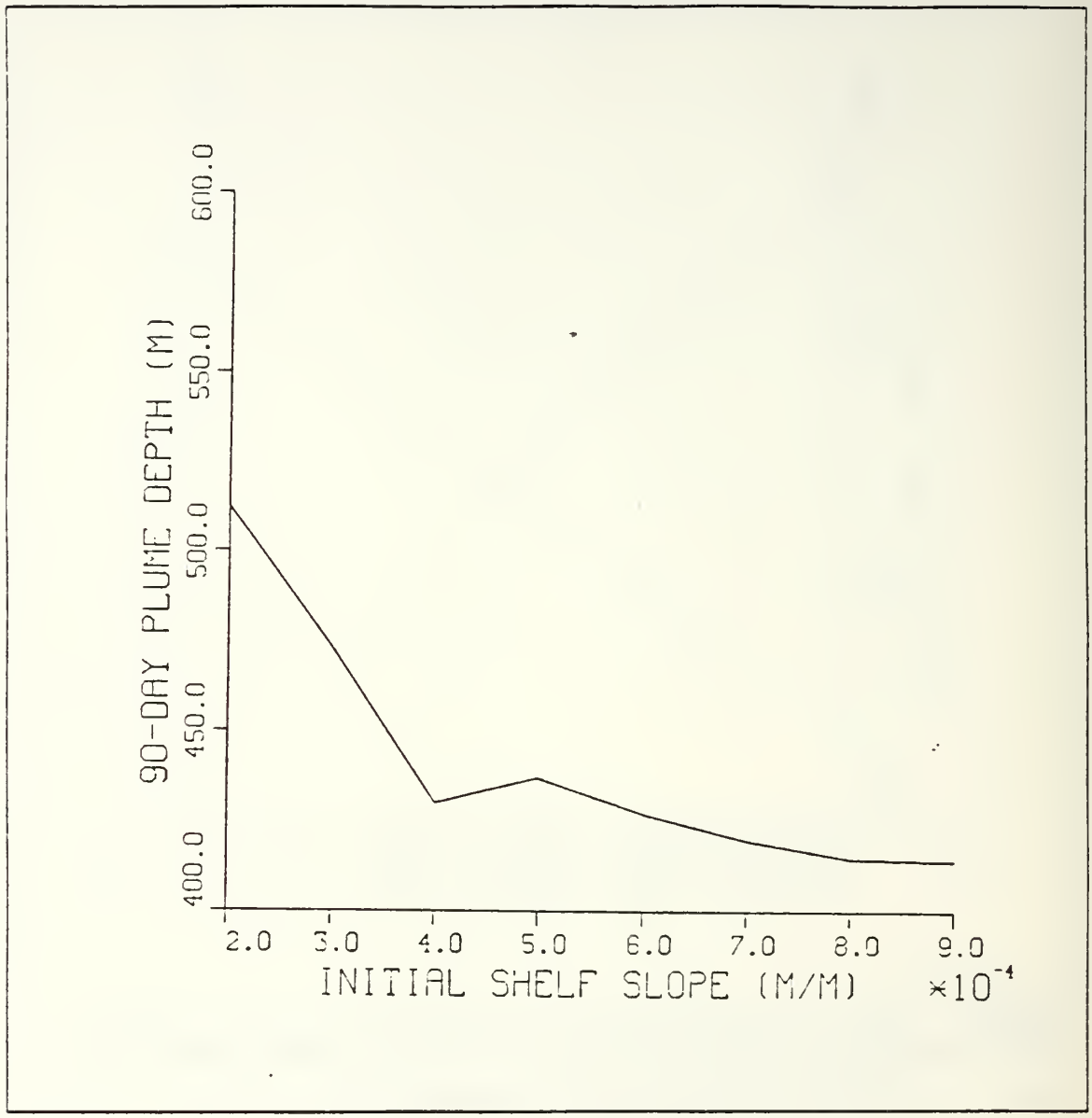

Figure 9. **This figure shows the effect of the initial shelf slope on the 90-day plume depth:** Due to the entrainment parameter being a function of slope, a steeper slope results in higher entrainment of ambient water, thus more rapid loss in negative buoyancy.

weakened initial stratification with $N^2 = 2.0x10^{-4}$ sec^2. The short length of time and space which the plume is exposed to this layer is probably the cause of its diminished impact on the 90-day plume depth.

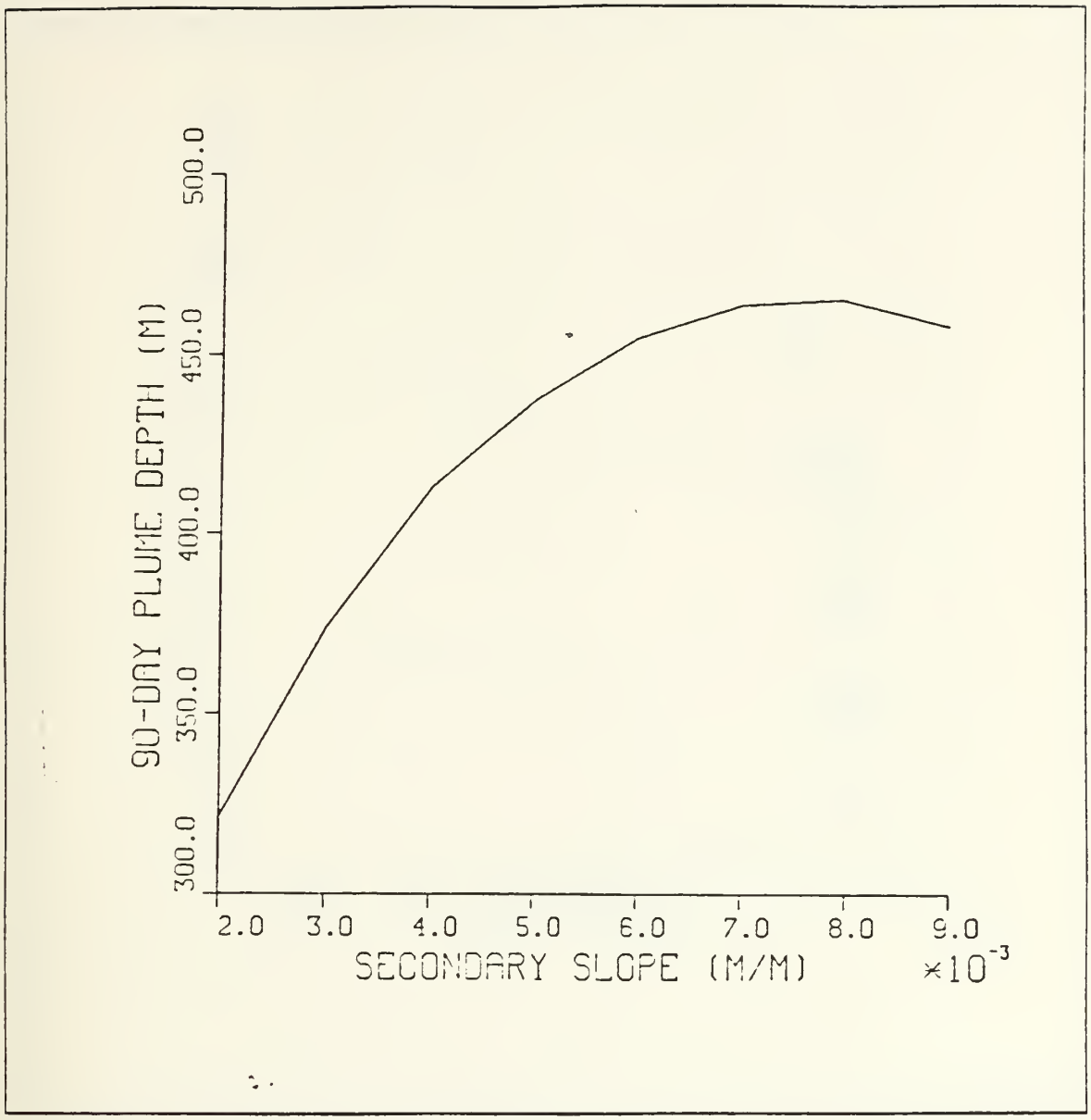

Figure 10. The effect of varying the secondary slope on the 90-day plume depth: Even with a higher entrainment rate, the plume reaches a deeper depth with a steeper slope, due to the physical boundary of the ocean bottom.

On the contrary, Figure 13 on page 28 shows the dramatic difference in the 90-day plume depth with small changes in the Brünt-Väisälä frequency in this 245 meter thick layer. Additionally, if the second layer's thickness is decreased, the plume will penetrate

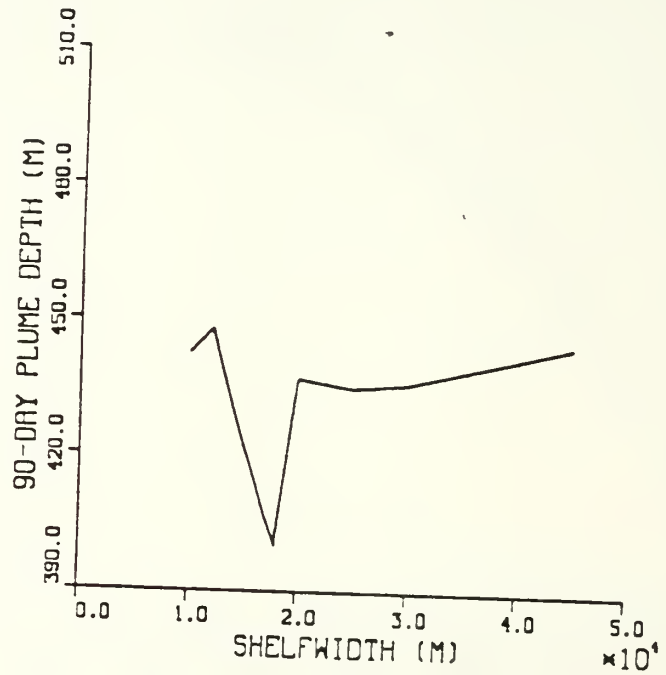

Figure 11. **The effect of varying the shelf width (after the 45 m isobath) on the 90-day plume depth:** Varying the shelf width has little effect on the 90-day plume depth.

to deeper depths. This is illustrated in Figure 14 on page 29. Note the discontinuity in the slope of the curve is caused when the plume no longer pentrates the second layer. Next, the standard case is compared in detail with a "submarine canyon" simulation.

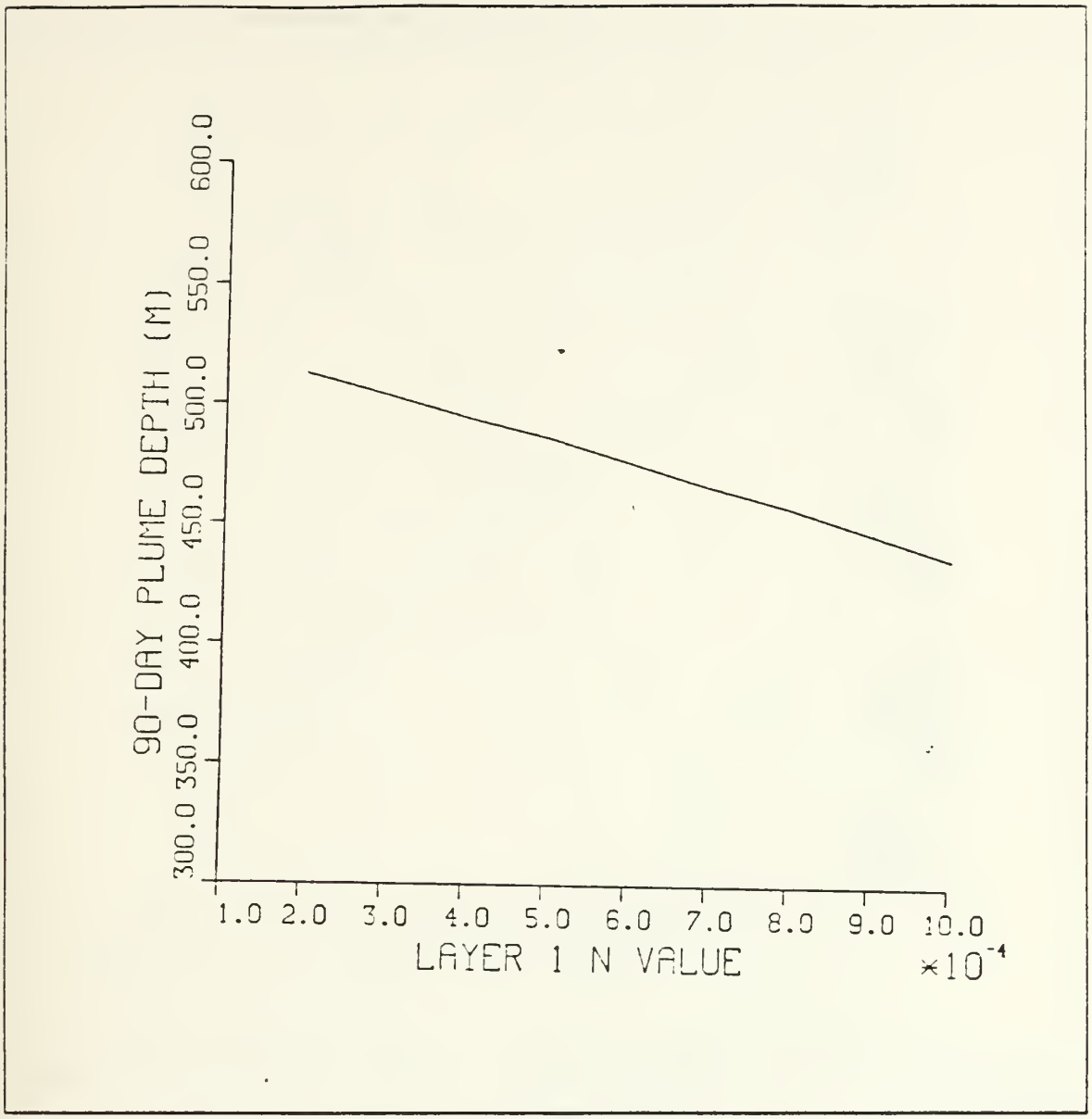

Figure 12. The effect of varying the initial pycnocline strength on the 90-day plume depth: The initial pycnocline, between 45 and 55 meter depths, has a small effect on the 90-day plume depth due to the small thickness of this layer.

C. THE "SUBMARINE CANYON" CASE

The "submarine canyon" case is a modification of the standard case using a steeper secondary slope, lower Layer 2 Brünt-Väisälä frequency value, and a decreased Layer 2

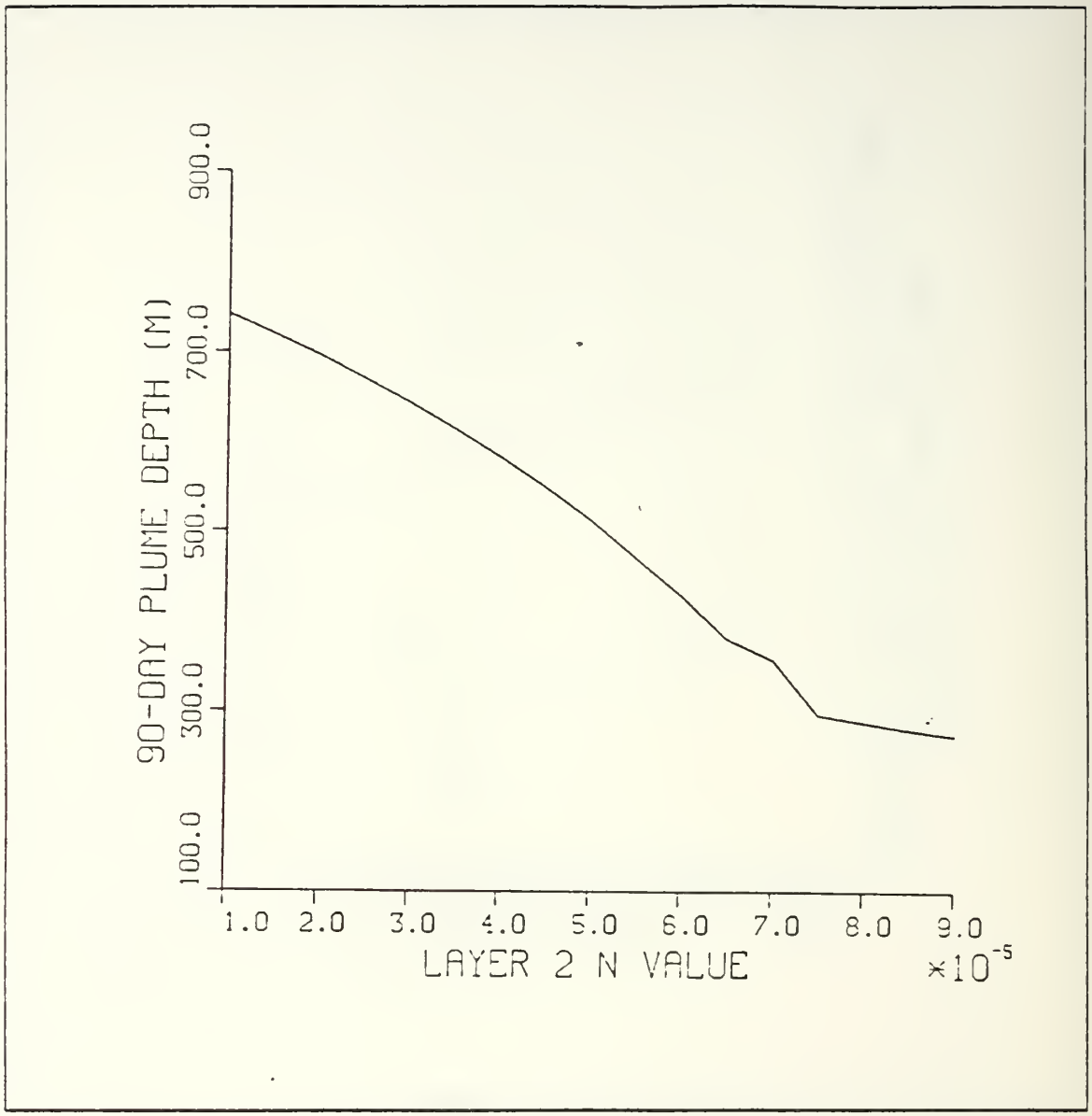

Figure 13. The effect of varying Layer 2 Brünt-Väisälä frequency on the 90-day plume depth: Due to the plume's longer exposure time in this layer, changes in Brünt-Väisälä frequency tend to have a more dramatic effect on the vertical motion of the plume.

thickness. In addition, the angle β, is forced to the initial value of 29 degrees to simulate the steering of the plume by topography. The initial values used in the "submarine canyon" case are shown in Table 5 on page 31. Forcing the angle β towards its initial

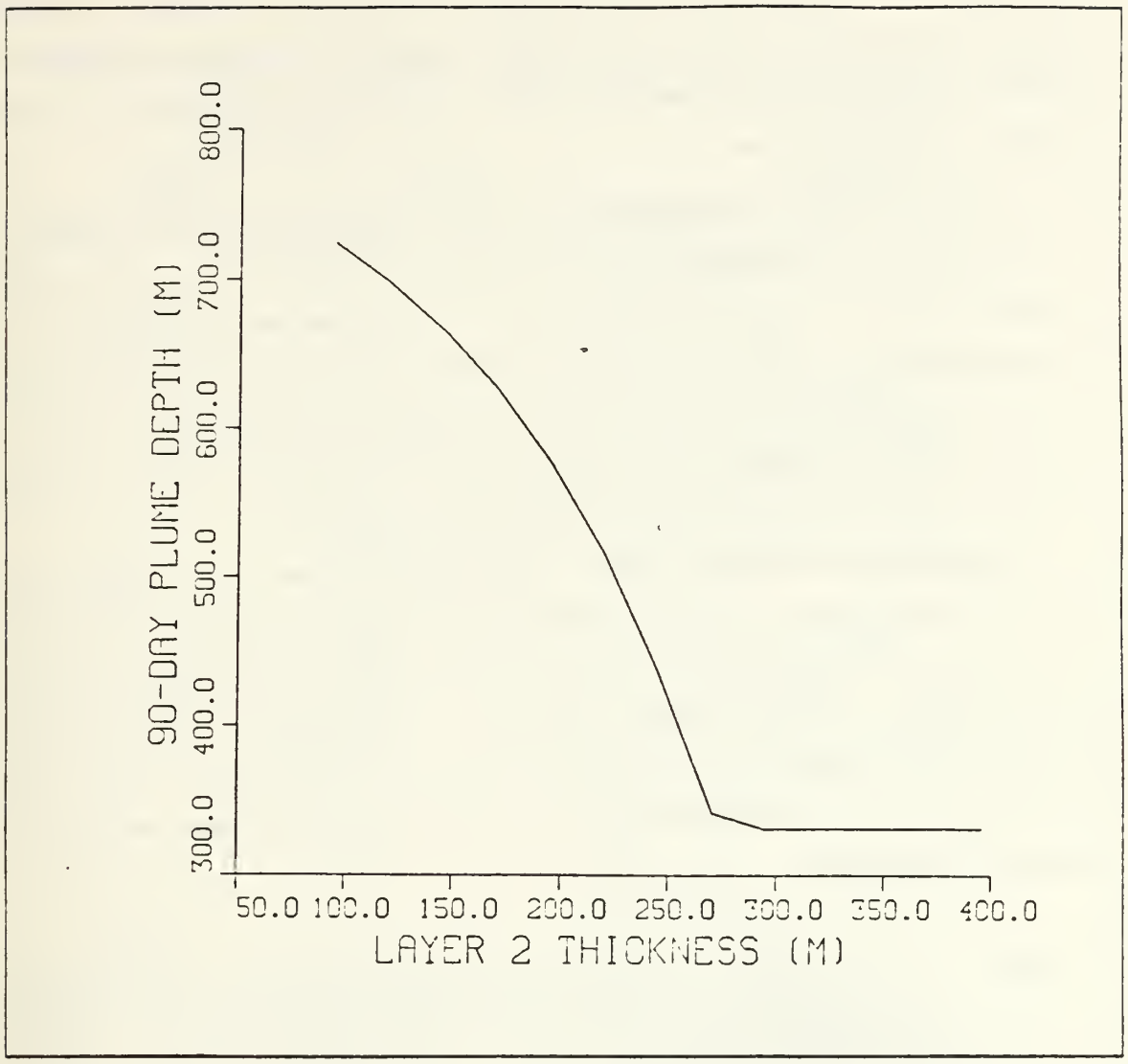

Figure 14. Decreasing Layer 2 thickness results in a deeper penetrating plume: As the plume can no longer penetrate Layer 2, due to its thickness, the 90-day plume depth becomes constant.

value results in the plume travelling down the Y axis further and less down the X axis. Of course, the value chosen for forcing β will alter the X-Y flow path of the plume. The flow path of the "submarine canyon" case is seen in Figure 15 on page 32. The plume, descends to a depth of over 1300 meters in 90 days, has moved 207 kilometers alongshore and 160 kilometers off-shore. In Figure 16 on page 33, the "submarine canyon" plume is seen to reach a maximum velocity of 0.36 m s whereas the standard case plume

has a maximum velocity of 0.30 m/s (Figure 3 on page 17). The effect of increased slope, the angle β, and velocity on entrainment is seen when comparing the volume flux of the "submarine canyon" plume (Figure 17 on page 34) and the standard case plume (Figure 18 on page 35).

D. RESULTS USING OBSERVED TEMPERATURE AND SALINITY FIELDS

The values for this experiment are the same as the standard case except the Brünt-Väisälä frequency is computed using observed values of temperature and salinity. The temperature and salinity records are from Ostlund (1987) and Aagaard et al. (1981) which were taken in the Canadian Basin. The results of the experiment are shown in Table 4. The 90-day plume depth and maximum velocities are very similar to the results from the Layer 2 Brünt-Väisälä frequency sensitivity experiment.

In an attempt to model a current as observed in Aagaard et al. (1985), a plume width of 20 kilometers was used together with a steep secondary slope and the temperature salinity fields reported in Aagaard et al. (1981). The plume's velocity with increasing depth is shown in Figure 19 on page 36. Aagaard et al. (1985) reported a 25 kilometer wide, 15 meter deep plume with a mean velocity of 0.45 m/s. The simulation yields a velocity of 0.30 m/s before the shelf break and 0.92 m/s while descending the steep secondary slope.

Table 4. THIS TABLE COMPARES SOME RESULTS FROM USING ACTUAL T-S RECORDS: The AIWEX-2 and AIWEX-8 stations are from Ostlund(1987) and the third record is taken from Aagaard et al. (1981).

Variable	AIWEX-2	AIWEX-8	Aagaard
V_{max} m/s	.397	.389	.395
90-day depth, m	217	213	305
X distance, km	311	312	363
Y distance, km	380	375	478

Table 5. **INITIAL VALUES USED FOR THE "SUBMARINE CANYON" CASE:** The highlighted values are those parameters which differ from the standard case.

Variable	Value	Definition
T_{air}, °C	-15.	air temperature
T_w, °C	-1.8	water temperature
V_{air}, $m\ sec^{-1}$	15.	wind velocity
V_i, $m\ sec^{-1}$	3 % V_{air}	ice floe velocity
H_i, m	.2	frazil collection thickness
σ, $Wm^{-2}deg^{-4}$	$5.67x10^{-8}$	Stephan-Boltzmann constant
e_a	0.95	emissivity of the air
ρ_a, kgm^{-3}	1.30	air density
ρ_w, kgm^{-3}	$1.026x10^{3}$	seawater density
ρ_i, kgm^{-3}	$0.95x10^{3}$	ice density
C_h	$2.0x10^{-3}$	sensible heat coefficient
C_a, $Jdeg^{-1}kg^{-1}$	1004	specific heat of air
Q_{la}, Wm^{-2}	301	longwave radiation upward
L, Jkg^{-1}	$3.34x10^{5}$	latent heat of fusion
b_0, m	10.	flow thickness
w_0, m	1000.	flow width
V_0, $m\ sec^{-1}$	.04	flow speed
β, degrees	29	flow direction
f, sec^{-1}	$1.38x10^{-4}$	Coriolis parameter
N, sec^{-1}	0.0316	Brünt-Väisälä frequency, layer 1
N	0.006286	**Brünt-Väisälä frequency, layer 2**
ΔZ_2, meters	145	**Layer 2 thickness**
N	0.001	Brünt-Väisälä frequency, layer 3
θ_1	$0.5x10^{-3}$	initial bottom slope
θ_2	$9x10^{-3}$	**secondary bottom slope**
K	0.01	drag coefficient
E	$0.072 \sin\theta \sin\beta$	entrainment coefficient
$\bar{S}$, ppt	32.5	initial shelfwater salinity
S_i, ppt	7.0	Salinity of frazil ice

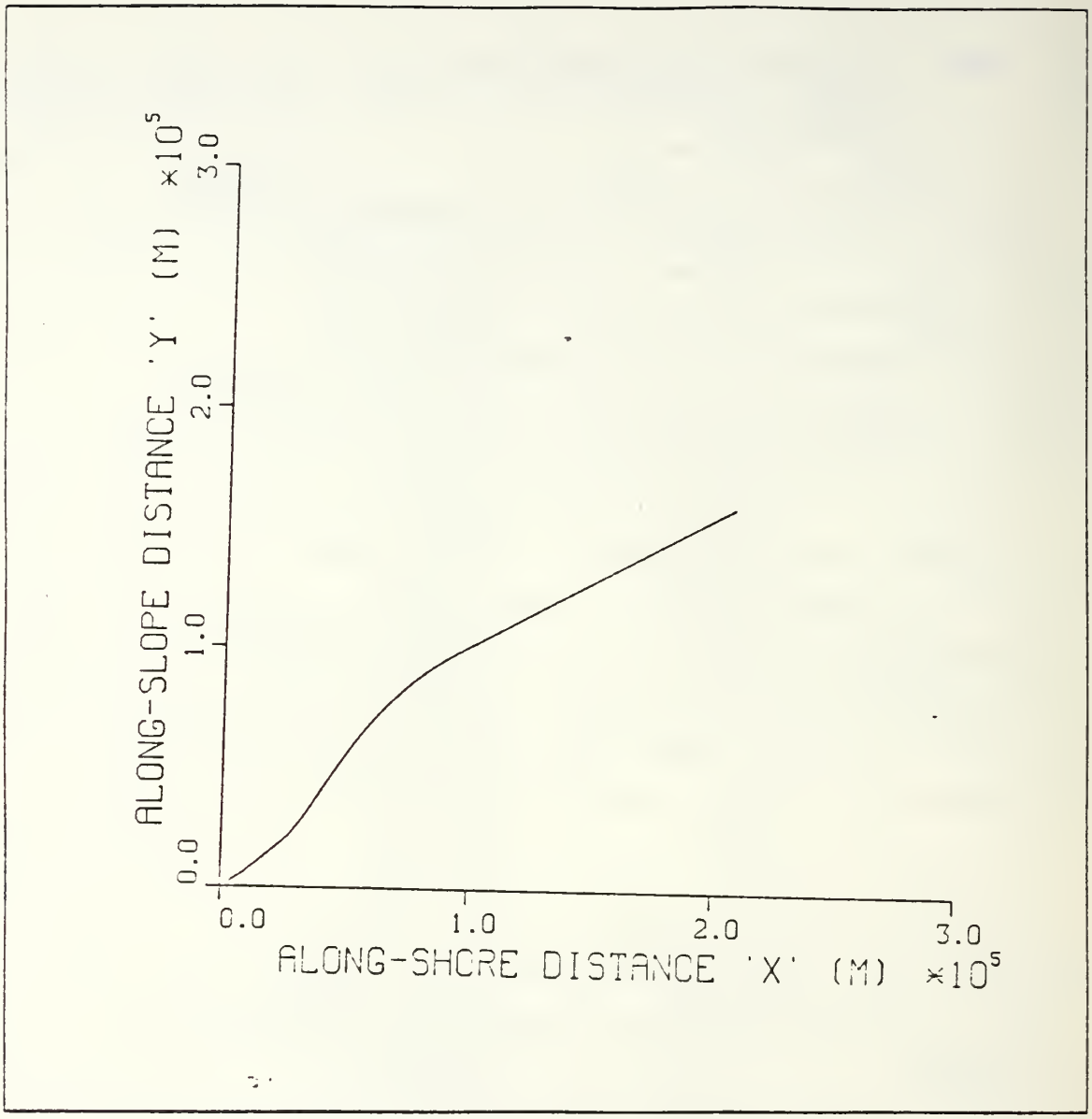

Figure 15. The "submarine canyon" plume's flow path: The plume's flow path is forced to the initial β value to simulate the topographic steering within a submarine canyon.

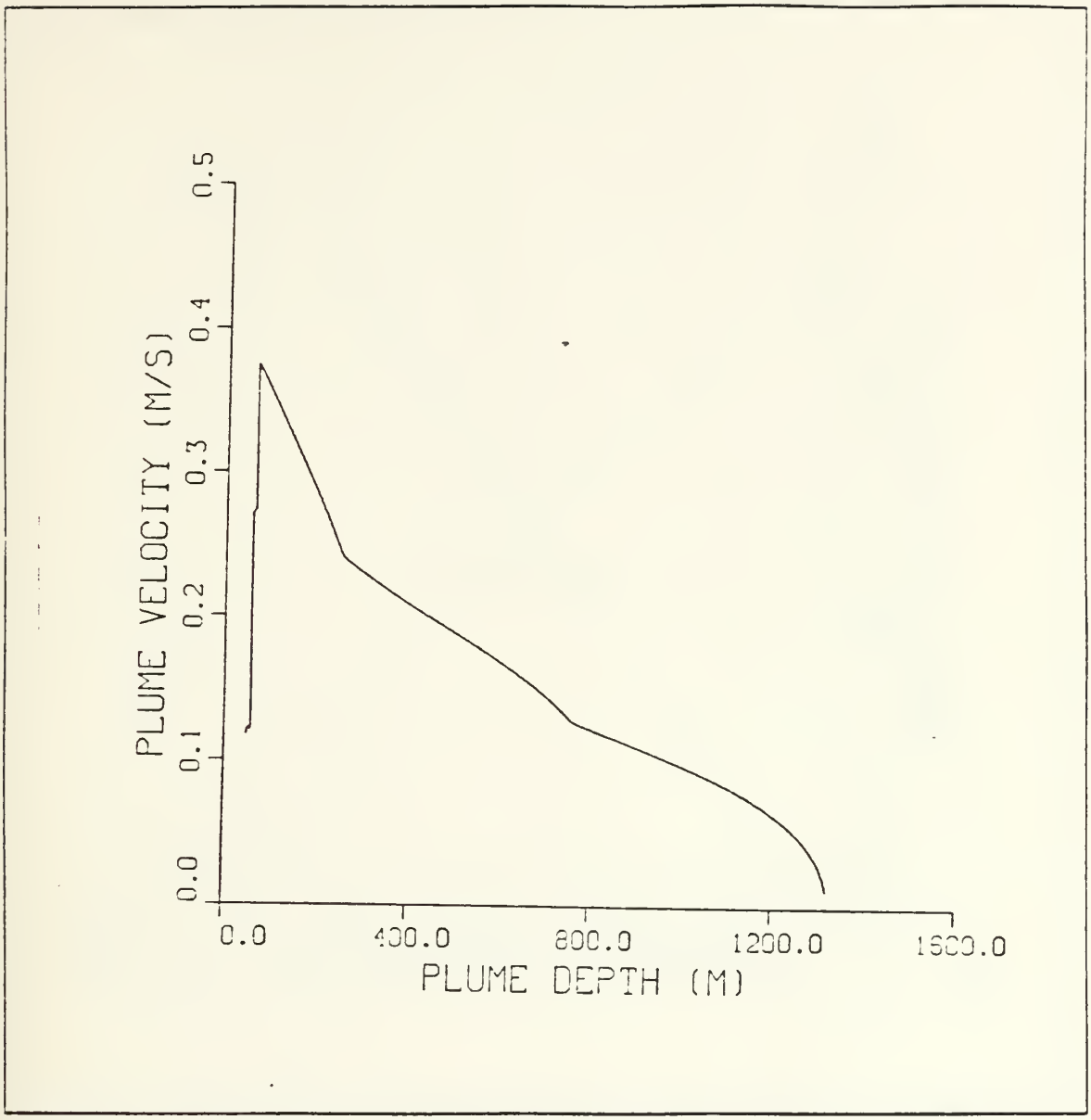

Figure 16. The velocity of a "submarine canyon" plume with increasing depth: The plume has the characteristic "jump" in velocity after the shelf break where it reaches a maximum velocity of 0.36 m/s.

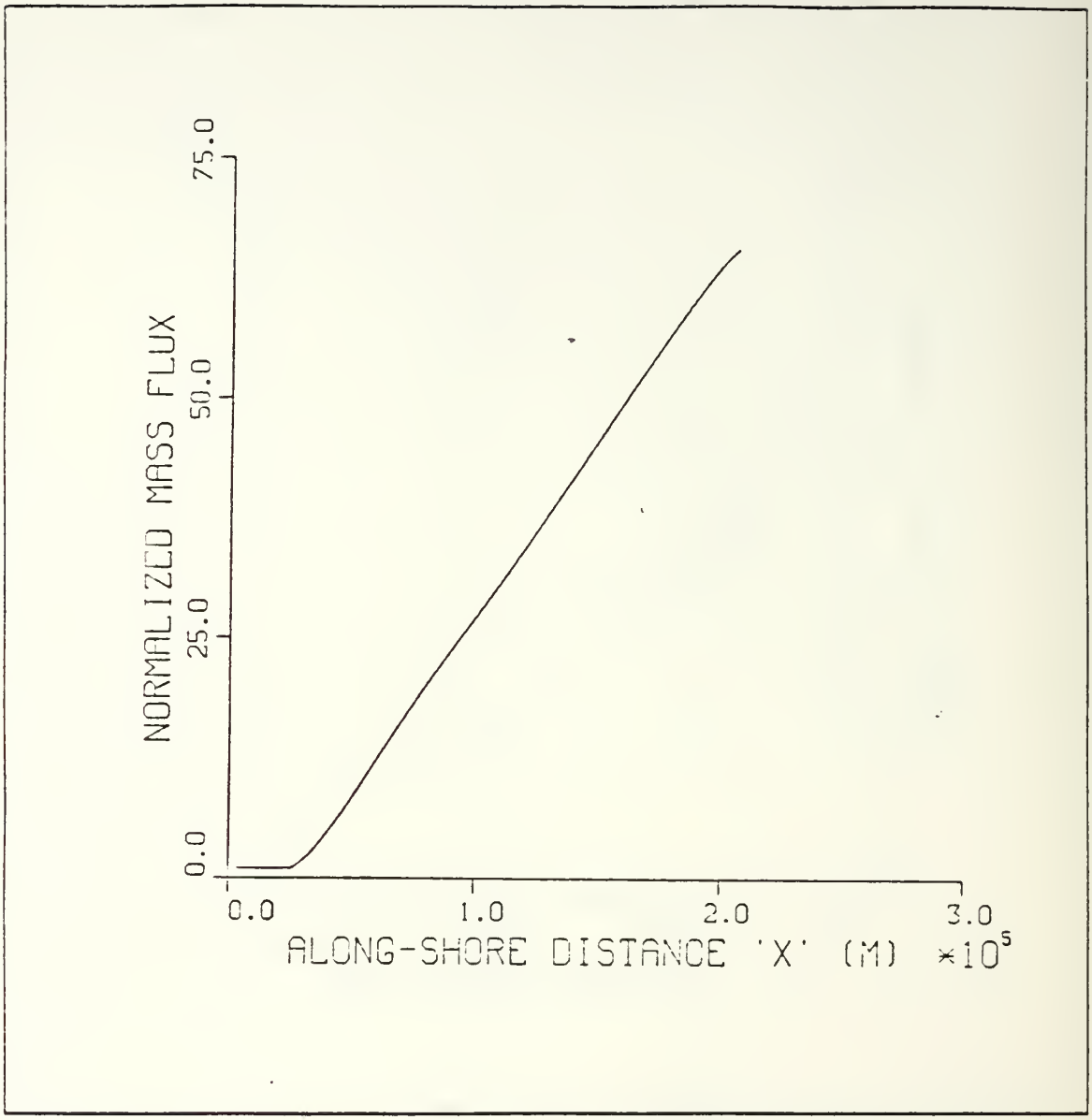

Figure 17. **The normalized mass flux of the "submarine canyon" plume:** The plume increases in mass by over 6800% indicating only 1 5% of the water reaching the deeper depths is shelf water.

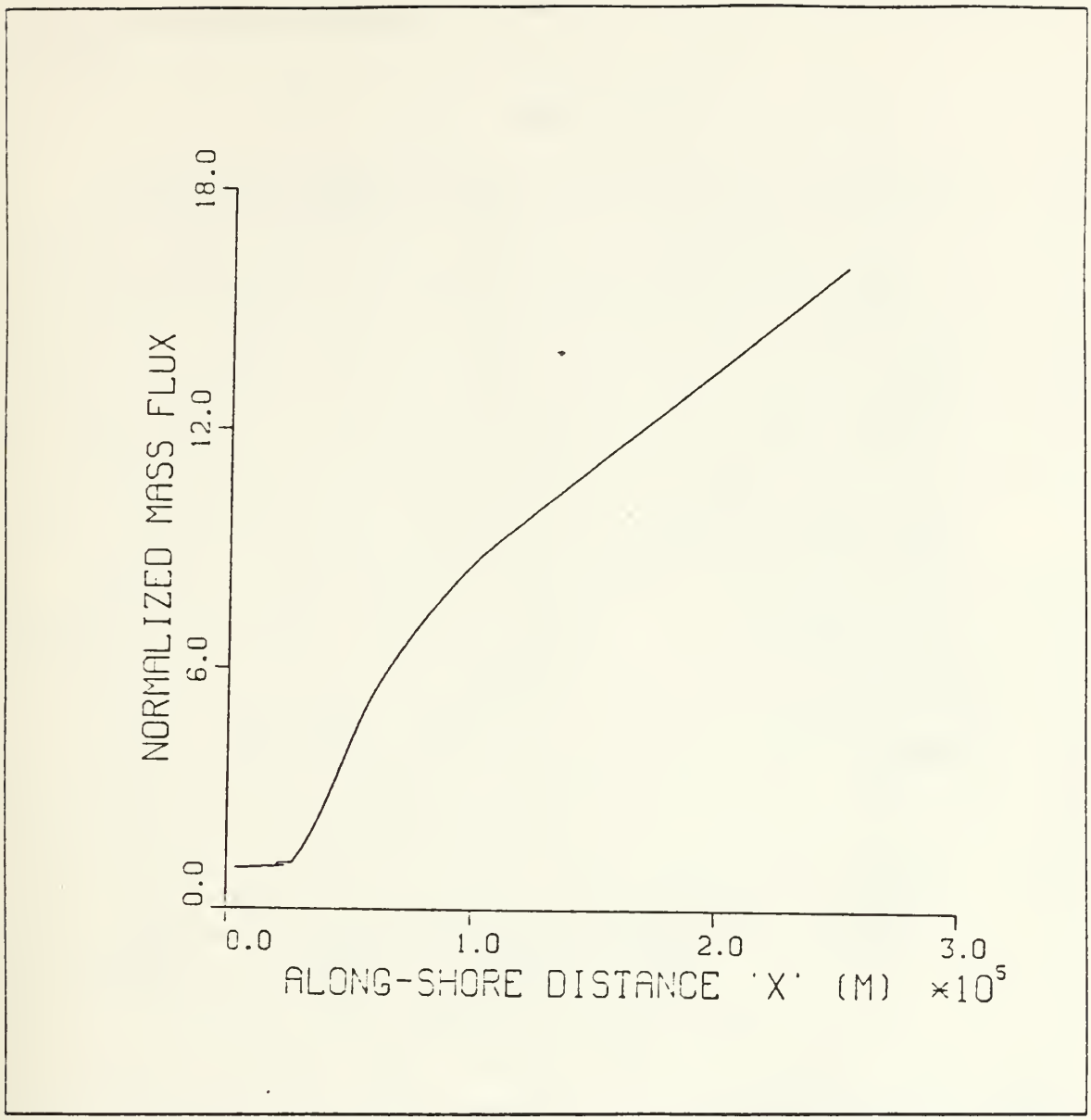

Figure 18. The normalized mass flux of the standard case plume: The standard case plume .

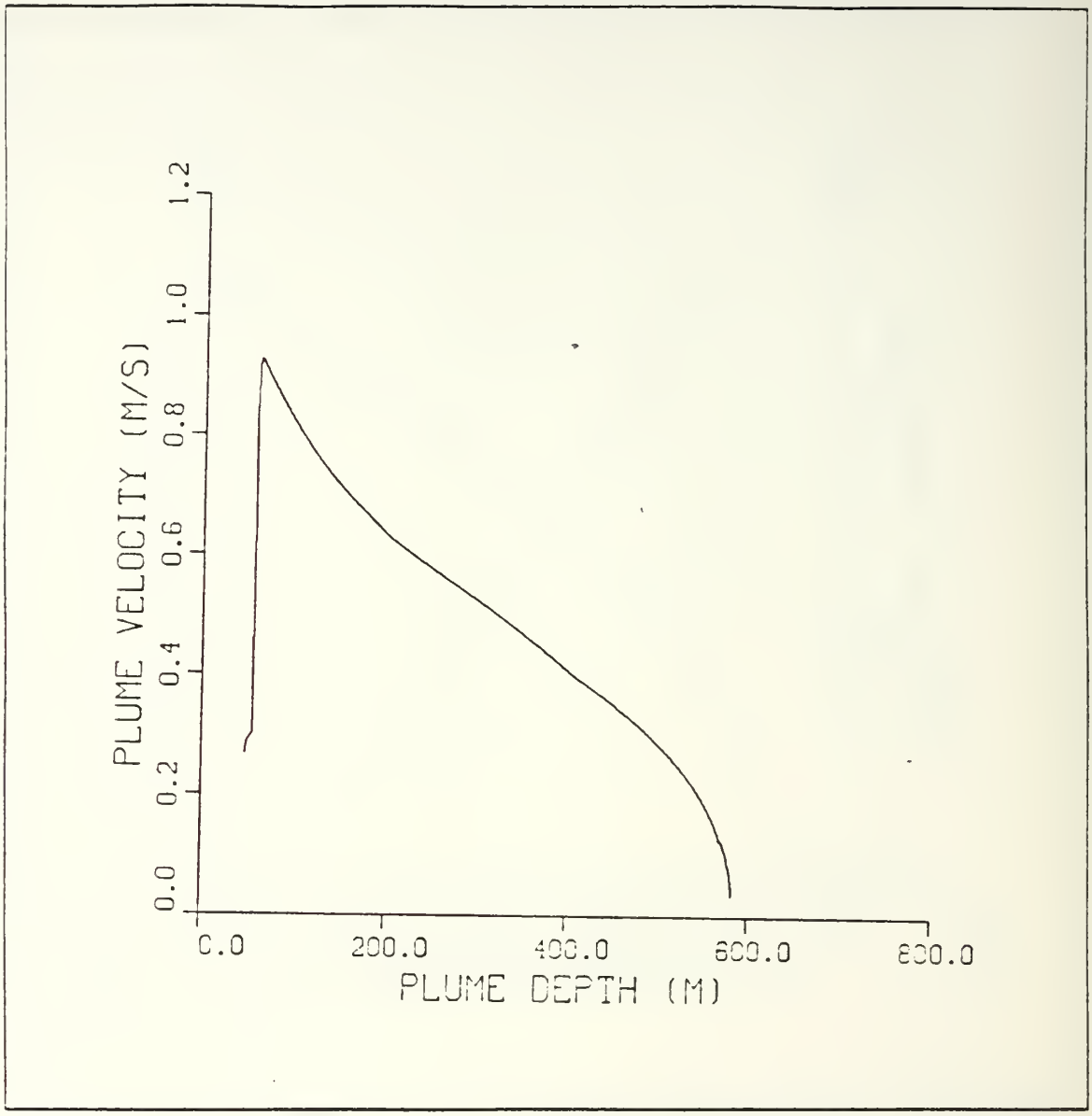

Figure 19. Velocity shown with depth of a 20 kilometer wide plume: This figure shows a wider plume can penetrate deeper than the narrower 1 kilometer plumes used in the previous experiments.

IV. DISCUSSION

This paper has attempted to provide a mechanism in which high salinity, low temperature water is produced and transported off the continental shelves into the Arctic halocline or deeper depths. The environmental parameters which affect the production and transport of this cold, salty water were examined, resulting in the conclusion that a polyna can produce water with a salinity greater than 34.5 ppt near the freezing point which can be transported via gravity flow plumes. The results show deeper penetrations to depths greater than 700 meters is possible depending on the set of environmental parameters. This indicates polyna-produced high density plumes may also be responsible for the ventilation of the deep Arctic Basins, specifically the Canadian Basin.

Ostlund et al. (1987) placed the residence time of Canadian Basin Deep Water between 500 and 800 years. Using the mixing ratio of 2:1 (shelfwater to intermediate water) from Aagaard et al. (1985), shelf water with a salinity of 35.1 ppt requires an off-shelf flux of approximately .0063 Sv to ventilate the Canadian Basin in 800 years. The results from the 20 kilometer wide plume experiment give an annualized flux of 0.0035 Sv. In other words, an average of about two such events per year where polyna-produced plumes penetrate below the temperature maximum over the past 800 years could account for the ventilation of the Canadian Basin. Furthermore, Ostlund et al. (1987) states that the deep water probably consists of much less than 10% shelfwater and would have to be a salinity of 36.15 ppt. The "submarine canyon" case shows the plume reaching a depth of over 1300 meters consisting of only 1.3% shelfwater at this depth. Table 3 on page 19 shows under extremely cold conditions, a salinity value of 36.23 ppt can be achieved with this model. Therefore, it is reasonable to expect that polyna-produced saline water may significantly contribute to the ventilation of the Canadian Basin.

Climatological variations which would affect the number of deep penetrating plumes are worthy of discussion. Besides the major periods of global ice ages and their counterpart warm eras, there have been recorded several shorter cold and warm epochs. These shorter periods coincide with weak and strong wind circulation, respectively. In the 20th century, both a warm period lasting about 20 years and a colder period beginning around 1950 have been recorded. In each of these two eras, there has been a sudden outflow of surface layers from the Arctic Ocean. Increased ice flow was recorded

in 1938 around Iceland during the warm period, while an increased flow of cold, low salinity water reached Iceland from the Arctic in the 1960's. Removal of the colder, fresher surface layer from the Arctic Basin would reduce the vertical temperature and salinity gradients resulting in a less stable vertical structure for the ocean. In effect, an environment similar to reducing the model's Layer 2 Brünt-Väisälä frequency and reducing the Layer 2 thickness may occur, enhancing deep plume penetrations. In addition to possible weakening of the vertical structure, removal of the ice cover leaves large areas of open water where heat is more readily removed from the ocean. In these large areas of open water, frazil ice grows rapidly and abundantly to increase the brine rejected into the water column. In the warm period of the early 20th century, the extent of the Arctic's semi-permanent ice pack was greatly reduced (up to 10%) between 1920 and 1938. The reduction in the semi-permanent ice pack is attributed to higher ice removal rates (increased advection) due to the strong wind circulation of the period. In Ostlund et al. (1987), it is noted that the deepest waters in the Canadian Basin may be the remains of the warm climate which occurred around 1000 A.D. vice any cold epochs such as the "Little Ice Age" in the late 17th and early 18th centuries.

In summary, periods when Arctic wind circulation is strengthened resulting in open water due to rapid ice divergence coupled with a weaker vertical Arctic Ocean stability seems to be the most conducive environmental scenario for deep plume penetrations to provide the additional salt source in the Canadian Basin.

In Killworth and Smith (1984), the heat diffusivity constant, κ , required to achieve steady state balances requires some peculiar changes in magnitude with increasing depth. A value of $\kappa \simeq 3 \times 10^{-6} m^2 s^{-1}$ is established to achieve a steady balance between the non-turbulent shelfwater plume used in Killworth and Smith (1984) and the region where the plume interleaves (note: the density of this plume is based on the brine rejection due to a single year's ice growth over a continental shelf of 50 meters average depth). To properly supply the East Greenland current outflow, κ was required to be $\simeq 3 \times 10^{-5} m^2$ sec^{-1}. And finally, to balance the inflow of warm Atlantic water and upward advection of heat, κ at this level was required to be $\simeq 1.2 \times 10^{-4} m^2$ sec^{-1} If the normalized mass flux of the turbulent plume model was to be used as a gauge to understand the turbulent diffusion, this thesis would present some interesting results. In Melling and Lewis (1982), the normalized mass flux was of order $\simeq 10^0$. In the standard case, the normalized mass flux was of order $\simeq 10^1$. The "submarine canyon" case had a mass flux of order $\simeq 10^2$. Could it be that the three above cases provide a insight into the missing

physics so stated in Killworth and Smith (1984)? Some other missing physics may be the double diffusion process as outlined in Carmack and Aagaard (1973) and the breaking of internal waves (Perkin and Lewis, 1978). Aagaard et al. (1985) suggests the incorporation of turbulent plume dynamics into the "filling box" model of Killworth and Smith (1984). A mechanism providing a specific low temperature, high salinity water source has been developed in this paper. Although the mechanism is episodic, as suggested Aagaard et al. (1985), (Killworth and Smith (1984) had earlier used the term "spasmodic"), due to the dependence on environmental variables, flux rates of this highly saline water can be estimated from renewal times of the Canadian Basin. The problem of incorporating the turbulent plume in the "filling box" model may be tackled, but is beyond the scope of this paper.

The maintenance of the Arctic halocline by the mechanism presented in this study alone would require many times the number of active polynas producing saline shelfwater. Using the 3:2 mixing ratio proposed by Aagaard et al. (1981), a minimum of 2.5 Sv production rate of cold, saline shelfwater was determined necessary to replenish the halocline over a period of 10 years. With the flux rate of the 20 km wide plume (.0035 Sv), the individual mechanism modelled in this paper would require 200-300 coastal polynas producing 2-3 high salinity, low temperature plumes per year to maintain the Arctic halocline. Although 200-300 such polynas may be thought prohibitive, areas of open water which exist during the onset of freezing temperatures in the late fall, as well as leads which continue through winter over as much as 10% of the ice pack, could provide a rapid source of salt to help overcome the summertime salinity gradient. In times of strong vertical structure, these polyna-produced plumes can transport low temperature, high salinity water into the Arctic halocline. Overall, the polyna seems to be an important source of brine which may help maintain the Arctic halocline and ventilate the deep basins.

REFERENCES

Aagaard, K., 1981. On the deep circulation in the Arctic Ocean. *Deep-Sea Research*, **28**, 251-268.

Aagaard, K., L. K. Coachman, and E. Carmack, 1981. On the halocline of the Arctic Ocean. *Deep-Sea Research*, **28**, 529-545.

Aargaard, K., J. H. Swift, and E. C. Carmack, 1985. Thermohaline circulation in the Arctic Mediterranean seas. *Journal of Geophysical Research*, **90**, 4833-4846.

Bo Pedersen, F., 1980, Dense bottom currents in a rotating ocean. *Journal of Hydraulics Division*, **106**, 1291-1308.

Carmack, E. and P.D. Killworth, 1978, Formation and interleaving of abyssal water masses off Wilkes Island, Antarctica. *Deep-Sea Research*, **25**, 357-369.

Carmack, E. and K. Aagaard, 1973, On the deep water of the Greenland Sea. *Deep-Sea Research*, **20**, 687-715.

Cox, G. F. N. and W. F. Weeks, 1974, Salinity variations in sea ice. *Journal of Glaciology*, **22**, 853-873.

Helland-Hansen, B., and F. Nansen, The Norwegian Sea: Its physical oceanography based upon the Norwegian researches, 1900-1904. *Rep. Norw. Fish. Mar. Invest.*, **2**(1), 1909.

Killworth, P. D., 1977, Mixing on the Weddell Sea continental slope. *Deep-Sea Research*, **24**, 427-448.

Killworth, P. D., and J. M. Smith, 1984, A one-and-a-half dimensional model for the Arctic halocline. *Deep-Sea Research*, **31**, 271-293.

Lamb, H. H., **Climate: Past, Present, and Future, Volume 1**, pp. 256-263, Methuen and Co., LTD, 1972.

Melling, H., and E. L. Lewis, 1982, Shelf drainage flows in the Beaufort Sea and their effect on the Arctic Ocean pycnocline. *Deep-Sea Research*, **29**, 967-986.

Millero, R. J. and A. Poisson, 1981, International one-atmosphere equation of state of seawater. *Deep-Sea Research*, **28**, 625-629.

Nansen, F., Northern waters: Captain Roald Amundsen's oceanographic observations in the arctic seas in 1901, *Nor. Vidensk. Acad. Kl. Skr. Mat. Naturvidensk. Kl.*, **1(3)**, 1906.

Ostlund, H. G., G. Possnert, and J. H. Swift, 1987, Ventilation rate of the deep Arctic Ocean from Carbon 14 data. *Journal of Geophysical Research*, **92**, 3769-3777.

Ou, H. W., 1988, A time-dependent model of a coastal polyna. *Journal of Physical Oceanography*, **18**, 584-590.

Pease, C., 1987, The size of wind driven coastal polynas. *Journal of Geophysical Research*, **92**, 7049-7059.

Perkin, R. G. and E. L. Lewis, 1978, Mixing in an Arctic fjord. *Journal of Physical Oceanography*, **8**, 873-80.

Schumacher, J. D., K. Aagaard, C. Pease, and R. B. Tripp, 1983, Effects of a shelf polyna on flow and water properties in the Northern Bering Sea. *Journal of Geophysical Research*, **88**, 2723-2732.

Smith, P. C., 1975, A streamtube model for the bottom boundary currents in the ocean. *Deep-Sea Research*, **22**, 853-874.

Sverdrup, H. U., 1929, The waters on the north Siberian shelf. *The Norwegian North Polar Expedition with the "Maud", 1918-1925. Scientific Results*, , **4(2)**., Bergen.

Weber, J. R., 1979, The Lomonosov Ridge Experiment: 'Lorex 79'. *EOS Transactions of the American Geophyisical Union*, 60, 715-720.

Weeks, W. F., and S. F. Ackley, 1982, The growth, structure, and properties of sea ice. CRREL Monograph 82-1, U.S. Army Cold Regions Research And Engineering Laboratory, pp. 130.

INITIAL DISTRIBUTION LIST

		No. Copies
1.	Defense Technical Information Center Cameron Station Alexandria, VA 22304-6145	2
2.	Library, Code 0142 Naval Postgraduate School Monterey, CA 93943-5002	2
3.	Chairman (Code 68Co) Department of Oceanography Naval Postgraduate School Monterey, California 93943-5000	1
4.	Chairman (Code 68Rd) Department of Meteorology Naval Postgraduate School Monterey, California 93943-5000	1
5.	Dr. Knut Aagaard NOAA/PMEL/MSRD 7600 Sandy Point Way , NE Seattle, Washington 98115	1
6.	Mr. Steve Ackley U. S. Army Cold Regions Research and Engineering Laboratory 10 Lyme Road Hanover, New Hampshire	1
7.	Maj. William C. Hill (Ret.) Route 3 Box 420 Sealy, Texas 77474	2
8.	Dr. Humphrey Melling Institute of Ocean Sciences P. O. Box 6000 9860 West Saanich Road Sidney, British Columbia Canada V8L 4B2	1
9.	Dr. H. Gote Ostlund Tritium Lab University of Miami Rosentiel School of Marine and Atmospheric Science 4600 Rickenbacker Causeway Miami, Florida 33149	1

10. Dr. Albert J. Semtner (Code 68Se) 5
Dept. of Oceanography
Naval Postgraduate School
Monterey, California 93943

11. Dr. Eddy Carmack 1
Institute of Ocean Sciences
P.O. Box 6000
9860 West Saanich Road
Sidney, British Columbia
Canada V8L 4B2

12. Dr. William Hibler 1
Thayer School of Engineering
Darmouth University
Hanover, New Hampshire

13. Dr. Carol Pease 1
NOAA/PMEL/MSRD
7600 Sandy Point Way, NE
Seattle, Washington 98115

14. Dr. James Swift 1
Scripps Institute of Oceanography
MLR Group, A030
La Jolla, CA

15. Dr. Peter Killworth 1
Robert Hooke Institute
Dept. of Atmospheric Physics
Parks Rd.
Oxford OX1 3PU England

16. Dr. Peter Wadhams 1
Scott Polar Research Institute
Cambridge, CB2 1ER, England

17. Dr. Robert Bourke (Code 68Bf) 1
Department of Oceanography
Naval Postgraduate School
Monterey, California 93943-5000

18. Dr. D. C. Smith, IV (Code 68Si) 1
Department of Oceanography
Naval Postgraduate School
Monterey, CA 93943-5000

19. Scientific Liaison Office 1
Office of Naval Research
Scripps Institute of Oceanography
La Jolla, California 92037

20. Dr. Bernard Lettau
Office of Polar Research
National Science Foundation
Washington, DC 20550

21. Dr. C. N. K. Mooers, Director
Institute of Naval Oceanography
Bldg. 1100, Room 311
NSTK Station
Bay St. Louis, Mississippi 39529

22. Mr. Michael Steele
Polar Science Center AP1
1013 NE 40th Street
Seattle, Washington 98105

23. Commading Officer
Naval Ocean Research and Development Activity
NSTL Station
Bay St. Louis, Mississippi 39522

24. Office of Naval Research (Code 1122P)
800 N. Quincy Street
Arlington, Virginia 22217

25. Chairman, Oceanography Department
U. S. Naval Academy
Annapolis, Maryland 21402